## REVIEW

Check for updates

# Carbon dots: a novel platform for biomedical applications

Mohammadreza Behi, [ID] *[ab] Leila Gholami,[c] Sina Naficy, [ID] [a] Stefano Palomba[bd] and Fariba Dehghani[a]

Carbon dots (CDs) are a recently synthesised class of carbon-based nanostructures known as zero-dimensional (0D) nanomaterials, which have drawn a great deal of attention owing to their distinctive features, which encompass optical properties (*e.g.*, photoluminescence), ease of passivation, low cost, simple synthetic route, accessibility of precursors and other properties. These newly synthesised nano-sized materials can replace traditional semiconductor quantum dots, which exhibit significant toxicity drawbacks and higher cost. It is demonstrated that their involvement in diverse areas of chemical and bio-sensing, bio-imaging, drug delivery, photocatalysis, electrocatalysis and light-emitting devices consider them as flawless and potential candidates for biomedical application. In this review, we provide a classification of CDs within their extended families, an overview of the different methods of CDs preparation, especially from natural sources, *i.e.*, environmentally friendly and their unique photoluminescence properties, thoroughly describing the peculiar aspects of their applications in the biomedical field, where we think they will thrive as the next generation of quantum emitters. We believe that this review covers a niche that was not reviewed by other similar publications.

[a]*School of Chemical and Biomolecular Engineering, The University of Sydney, Sydney, 2006, Australia. E-mail: mbehi@kth.se*

[b]*Institute of Photonics and Optical Science, School of Physics, The University of Sydney, Sydney, NSW 2006, Australia*

[c]*Nanotechnology Research Center, Pharmaceutical Technology Institute, Mashhad University of Medical Science, Mashhad, Iran*

[d]*The University of Sydney Nano Institute, The University of Sydney, Sydney, NSW 2006, Australia*

## 1. Introduction

The fast progress of novel nanomaterials development creates more efficient platforms in different fields, leading to applications in the biomedical, energy, photonics, material, environmental and catalysis industries.[1–5] Despite the countless advantages demonstrated by nanomaterials, their exploitation is limited because, in the majority of cases, they require toxic chemical reagents for their synthesis. Hence, they are not considered to be environmentally friendly. Therefore, to

*Reza received his Professional Doctorate in engineering in 2014 from Technical University of Eindhoven (The Netherlands), and his PhD in cancer-diagnostics in 2018 from University of Sydney (Australia). He is a skilled research professional with 10 years of experience in multidisciplinary institutions and projects across Europe (KTH, TU/e, ESADE, UPC, NANOHEX, SUNCOOL) and Australia (The University of Sydney). His research focuses on Nanobiosensor technology, Wearable Sensors & IoT, 3D Printing, MEMS and Energy Technology.*

*Leila earned her PhD in Molecular Medicine in 2018 from Mashhad Medical University of Sciences Iran). She is currently a postdoctoral researcher at the Nanotechnology Research Center, Institute of Pharmaceutical Technology at Mashhad University of Medical Sciences. Her research contributions have been to design, synthesize and modify efficient non-viral polymeric vector and different nano-carriers for drug and gen delivery for different biomedical applications.*

eliminate hazardous chemical reagents, great endeavours have been made to design and introduce reproducible, environmentally friendly nanostructures.[5,6]

Carbon dots (CDs) are zero-dimensional carbon nanomaterials (1–10 nm) with unique optical properties and were introduced in the scientific community by Xu *et al.* in 2004.[7] CDs are mainly categorized by their chemical structure, which determines their peculiar properties. These new nanomaterials exhibit $sp^2$ or $sp^3$ hybridization and usually are decorated with oxygen-based groups on their surface, as well as other chemical groups left from post-treatment processes.[8,9] Given their 3D quantum confinement and surface effects, CDs exhibit unique optical properties, such as electrochemiluminescence, photoluminescence (PL), and chemiluminescence.[10–16]

PL emission spectra of carbon dots can cover a spectral range from ultraviolet to visible and near infrared,[17] as a function of their intrinsic dimensions. Improving the manufacturing processes plays a critical role in the PL efficacy, spectral purity and stability which are critical for certain relevant applications.[18,19]

It is well-known that the quantum size effect and the surface nature of the CDs are two very influential factors on their PL characteristics. However, the precise mechanisms are still under debate and both, electron donor or acceptor, can create photoluminescence. Photoinduced CDs are both excellent electron donors and acceptors. Thus, they can be quenched efficiently by either electron acceptors or donors.[17]

Besides, the emission wavelengths can be adjusted by chemical components and the processes used for their synthesis. For instance, in the controlled thermal pyrolysis of citric acid and urea, the spectral emission peak of the generated CDs can be gradually changed by regulating the thermal-pyrolysis temperature and the ratio of reactants.[20] In contrast, fabricated CDs by a one-step hydrothermal process have been shown to display a broad band emission over the whole visible wavelength range.[21]

Relying on these exclusive optical properties and their intrinsic biocompatibility, CDs are competitive alternatives to well-known semiconductor quantum dots (SQDs), containing potentially toxic compounds and heavy metals.[22,23] Additionally, CDs offer excellent water solubility, high chemical and optical stability,[16] magnificent biocompatibility, and are cost-effective and environmentally friendly. The combination of these attributes makes CDs a promising candidate for numerous applications, such as fluorescent markers, bioimaging agents, photocatalysts, sensing, and optoelectronic devices.[24–29]

The difference in the structure of different CDs primarily stems from the synthesis process and raw materials used.[30] CDs are produced from a variety of synthetic or natural carbon sources.[31–33] Thus, a significant number of protocols have been developed for their fabrication, involving both natural and synthetic precursor strategies. Compared to synthetic carbon sources, the natural and sustainable carbon sources and

*Sina received his PhD in Materials Engineering in 2011 from the University of Wollongong (Australia). After 5 years of postdoctoral research at the Intelligent Polymer Research Institute and ARC Centre of Excellence for Electromaterials Science, Sina joined the School of Chemical and Biomolecular Engineering at the University of Sydney in 2016. His research focuses on materials development and the fabrication of flexible sensors and soft robotic systems.*

*A/Prof. Stefano Palomba is a Physicist in Experimental Nanophotonics. After earning a PhD degree in Nanoscale Physics (UK – 2007), he worked as a Postdoctoral Fellow in Professor Lukas Novotny's Nano-Optics group at the University of Rochester (USA) and in Professor Xiang Zhang's group at the University of California, Berkeley (USA). He is now the Director of the Nanophotonic and Plasmonic Advancement Lab (NPAL), the Deputy Director of the Institute of Photonics and Optical Science (IPOS) since 2015 and he is co-leading the Lab/Organ-on-Chip cluster in the NanoHealth Network (Sydney Nano Institute). His research focuses on linear, nonlinear and quantum nanophotonics and plasmonic including sensing and neurophotonics.*

*Fariba Dehghani completed her PhD from the University of New South Wales. She is currently a Professor in School of Chemical and Biomolecular Engineering at the University of Sydney and the director of Centre for Advanced Food Engineering. She leads a multidisciplinary bioengineering research team that focuses on developing technologies for nutritional food products and biomaterials, with particular emphasis on tissue engineering and regenerative medicine. She has an extensive collaborative research with industry for developing pragmatic, cost effective and environmentally sustainable solutions to a diverse range of issues, with the aim of improving human wellbeing.*

Table 1 A summary of review articles from the past eight years devoted to the synthesis, photoluminescence (PL) mechanism, and applications of CD

| Authors | Year | Reviewed synopsis | Ref. |
|---|---|---|---|
| Li *et al.* | 2012 | This article focuses on the synthesis of CDs, surface functionalization, PL properties, and their applications in photocatalysis, photovoltaic, energy and sensors. Moreover, the photo induced electron transfer ability and light-harvesting capability of CDs are discussed | 10 |
| Yang *et al.* | 2013 | This article reviews the hydrothermal, solvothermal, and microwave synthesis of fluorescent CDs and their sensing applications as nanoprobes for ions, organic and biological molecules and target gases. Furthermore, the application of CDs in cell imaging and drug delivery is discussed | 42 |
| Wang *et al.* | 2014 | In this article, the progress in the synthesis of CDs is summarized, focusing on various synthesis methods, size control, and modification strategies. Furthermore, the properties and applications of CDs have been reviewed, including their photoelectric properties, luminescent mechanism, and applications in biomedicine, optronics, catalysis, and sensing | 43 |
| Hong *et al.* | 2015 | This review article surveys the synthesis, functionalization, and biocompatibility of carbon nanomaterials and their progress in biological imaging and nanomedicine therapy | 48 |
| Zheng *et al.* | 2015 | This paper explores the problems associated with CDs, such as the broad emission spectrum, low quantum yield, and low-yield synthesis methods. It is concluded that most CDs emit in the green or blue spectral range. Meanwhile, excitation and emission at long wavelengths are particularly desired for deep tissue imaging | 44 |
| Zhu *et al.* | 2015 | This review article explores the synthesis methods and properties of three CDs and the advances in elucidating the PL mechanism of these materials | 45 |
| Cayuela *et al.* | 2016 | In this review, the decorated fluorescent dots serve as central nano scaffolds, which helps assemble and display one or more functions, such as targeting or sensing biomolecules and bio-imaging. They concluded that the efforts should be directed to design a multifunctional platform by controlling drug release, targeting, monitoring pharmacokinetics, and biodistribution. Although they are considered promising multi-modal phototherapeutic agents for enhanced cancer therapy in future clinical applications, further investigations are needed, particularly for carbon-based dots | 50 |
| Reiss *et al.* | 2016 | This article reviews the synthesis of semiconductor nanocrystals and colloidal quantum dots in organic solvents, emphasizing earth-abundant and toxic heavy metal-free compounds | 51 |
| Zhou *et al.* | 2017 | In this review article, the progress in imaging using CDs doped with heteroatoms (X-CDs) is summarized. The design strategies, doping species, properties, PL mechanism, and bioimaging applications are discussed | 52 |
| Namdari *et al.* | 2017 | This article describes the novel application of CDs for *in vivo* imaging and their potential for imaging tumours in the near future | 53 |
| Tuerhong *et al.* | 2017 | This review article highlights the progress made in polymer-based CDs, including the effect of polymers on the formation of CDs, their fabrication, and applications | 54 |
| Tao *et al.* | 2017 | This review article focuses on polymer-based carbon dots and summarizes their formation process, properties, and PL mechanism | 55 |
| Chen *et al.* | | In this article, graphene quantum dot-based nanohybrid materials are discussed in regard to their method of synthesis, physicochemical properties, and specific biocompatibility characteristics compared to other nanostructured materials | 56 |
| Das *et al.* | 2018 | This review article summarizes the synthesis methods of CDs made from natural sources. These include electrochemical synthesis, microwave, confined pyrolysis, or solution chemistry | 46 |
| Zhang *et al.* | 2018 | This review paper discusses the recent progress in the synthesis, characterization, and applications of CDs made from natural sources. The applications include bioimaging, solar cells, sensors, and catalysis | 47 |
| Chan *et al.* | 2018 | This review illustrates a series of various carbon dot-based sensors in terms of their sensing mechanism. In addition, these sensors' sensitivity and selectivity for detecting different elements comprising of heavy metals, cations, onions, and so forth are investigated | 57 |
| Ghosal *et al.* | 2019 | This review focuses on current methods of CDs preparation. It also evaluates the impact of synthesis methods and the fluorescence properties of CDs in the biomedical area, specifically focused on therapeutic platforms | 58 |
| Wagner *et al.* | 2019 | In this review paper, recent signs of progress and obstacles in the design of quantum carbon dot are discussed, and various approaches to improving the quantum yield stability by bioconjugation clearance are explained. Also, it provides a detailed overview of the distribution and toxicity of quantum dots | 59 |
| Yuan *et al.* | 2019 | In this review, in addition to general information about the synthesis methods of CDs and their optical properties, new insights are given at room temperature phosphorescence, delayed fluorescence properties, and their optoelectronic applications, such as light-emitting diodes, lasing, solar cells, and photodetectors. Additionally, obstacles faced in materializing these applications are discussed | 60 |
| Su *et al.* | 2020 | This article provides a comprehensive scope of CDs application in the bioimaging of normal and cancer stem cells and tumour cells, two-photon fluorescence imaging, *in vivo* imaging, biosensing, and different platforms of cancer therapy | 61 |

**Table 1** (*Contd.*)

| Authors | Year | Reviewed synopsis | Ref. |
|---|---|---|---|
| Koutsogiannis *et al.* | 2020 | This article focuses on the effects of CDs development methods and its bioimaging properties as a cancer theranostic agent | 62 |
| Goreham *et al.* | 2020 | This review article explicitly emphasizes the modifiable properties of CDs as a labelling agent for particularly extracellular vesicles tracking and their application in bioimaging and biosensing | 63 |
| Wang *et al.* | 2020 | In this article, the properties of semiconductor quantum dots produced *via* inorganic or organic modification methods are categorized. The pros and cons of various fabrication methods in relation to their function in the mechanical field of bioimaging and drug delivery are discussed | 64 |
| Liu *et al.* | 2020 | In this article, the authors evaluate and compare the properties of traditional quantum dots and carbon dots. They also present a bright scheme of physicochemical properties and methods of preparation, along with a novel outlook for the comprehensive identification of traditional quantum dots and carbon dots | 65 |

resources,[34–37] such as biomaterials[38,39] and food waste,[40] offer low or zero additional cost, high water solubility, and lower cytotoxicity.[40,41]

A number of review articles have thoroughly discussed the synthesis aspects of CDs in the past[10,42–45] and more recently.[46,47] Others have explored the biological aspects of CDs in applications, such as biomedicine and bioimaging.[43,48,49] Table 1 reports a summary of several review articles in the past eight years regarding CDs. Overall, most of the review articles have been dedicated to either the synthesis and characterization of CDs or their applications in the biomedical field.

This review article focuses more on the characterization and classification of CDs, mainly produced by natural sources, for biomedical applications. A brief introduction to carbon dots and different classes of CDs is first presented, followed by a discussion on various synthesis routes for the production of CDs (particularly from natural sources). The optical properties of CDs are then explored in details. Lastly, the progress made in the biomedical fields, specifically in three different areas of biomedicine, bioimaging and bio/chemo sensing, are outlined. To conclude, the future outlook and further recommendations on the field of interest are discussed (Fig. 1).
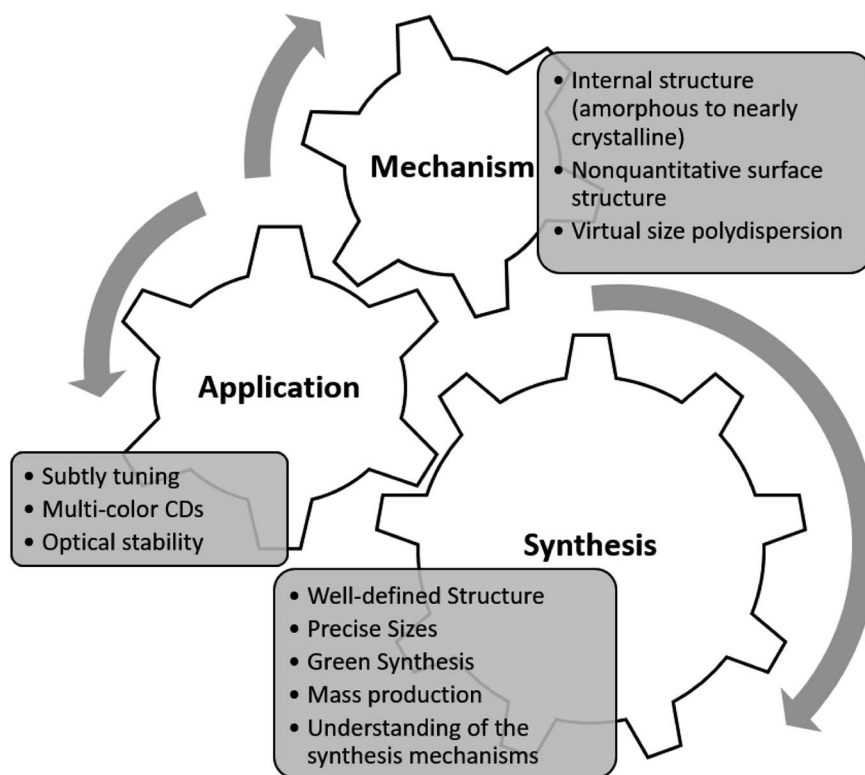


Fig. 1 The addressable areas of research for CDs.

# 2.  Carbon dots families

The families of CDs can be categorized into three sub-classes based on their origin and nature, namely carbon nanodots (CNDs), graphene quantum dots (GQDs), and polymer carbon dots (PCDs). Each sub-class of CDs exhibits a different set of surface chemistry, as depicted in Fig. 2, and consequently exhibit different optical properties.

## 2.1.  Carbon nanodots

Carbon nanodots (CNDs) are quasispheroidal carbonaceous nanoparticles of less than 10 nm in size. CNDs are carbon nanoparticles without a crystal lattice. Carbon nanoparticles with a crystal lattice are called graphene quantum dots (GQDs), which are discussed in the next section.[66] CNDs have been extensively studied to better understand the origin of their photophysical behaviour,[10,67–70] and to develop more efficient synthesis routes in which the size and surface chemistry can be finely tuned.[71–73]

Rhee and Kwon first developed a size-controlling synthesis process for CNDs where they used a "water-in-oil" emulsion as a nanoscale self-assembling platform.[74,75] Surfactant molecules encapsulated the formed micelles of water in an immiscible oil. The CNDs were then developed by elevating the temperature to 250 °C for 2 hours under argon. They also evaluated the effect of different temperatures (160 and 200 °C) to optimize CND production. Furthermore, the carbonization and capping process of CND were performed under the optimized temperature. It was found that the water-surfactant concentration could regulate the size of the micelles. Therefore, this method could offer size tenability with a narrow size distribution.

Rhee and Kwon also found that different-sized CNDs had non-identical band gaps and hence different PL behaviours. The PL peak blue-shifted by approximately 25 nm upon increasing the size of the CNDs from 1.5 to 3.5 nm. These results, which are opposite to what was expected from the quantum size effect, were further explained by sp$^2$ hybridisation exhibiting specific energy gaps due to bonding with oleylamine ligands that acted as auxochromes to reduce the energy gaps. As a result, large CNDs with relatively small ligand/sp$^2$ clusters had larger band gaps than small CNDs. Therefore, the broad absorption peak near 370 nm was obscured in large CNDs, and the maximum PL peak was shifted to 360 nm.

By employing different fabrication pathways, various functional groups, including highly polar groups, such as carboxyl (–COOH) and amine (–NH$_2$), are exploited for the surface modification of CNDs,[32,76,77] making them suitable for a range of biomedical applications, such as nanobiosensors. Such functional groups have different energy levels, resulting in a series of surface trapping states in CNDs that dominate the emission spectrum. A higher degree of surface oxidation or other effective passivation can result in more surface defects, resulting in a red-shifted emission. The modified CDs are extremely photoluminescent, either in suspension or solid-state. Their emission encompasses the visible spectral range and expands into the near-infrared; the latter property allows the dots to be utilized in biosensing applications.

## 2.2.  Graphene quantum dot

Graphene quantum dots (GQDs) are made of a single-layer carbon core connected to different chemical groups on the surface.[78,79] GQDs have received considerable attention in recent years because of their photostability,[80] small size,[81,82] biocompatibility,[80] highly tunable photoluminescence properties,[83,84] multi-photon excitation,[85] electrochemiluminescence,[64] ease of modification,[86,87] and chemical inertness.[88–90] Because of their small size and biocompatibility, GQDs can serve as an active carrier in bioimaging,[91–93] optical sensing,[94,95] and drug delivery,[96,97] while enabling visual monitoring of the drug release kinetics.[97] Moreover, their exceptional catalytic and physicochemical properties can be substantially utilized in various biomedical applications, further discussed in the following sections.

## 2.3.  Polymer carbon dots

Polymer carbon dots (PCDs) are fluorescent nanoparticles that are primarily made of macromolecules as the carbon source, where the carbon core is grafted with polymer chains on the surface.[78,79,98–102] The macromolecular carbon sources used for the production of PCDs are generally π-conjugated polymers, and the PL centres are attributed to the formation of the carbon core. After the π-conjugated macromolecules, the fluorophores are processed by dehydration, condensation, carbonization, or assembly routes.[103,104]

Their synthesis route governs the PL mechanism of PCDs. For instance, Liu et al. synthesised photoluminescent polymer nanodots (PPNDs) by a grass hydrothermal process. They reported that an enhancement in the reaction temperature resulted in a size reduction and a surge in the quantum yield. They revealed that their synthesised PPNDs also possessed a suitable sensitivity for detecting Cu(II) ions with a low detection limit of 1 nM in the water samples.[98]

Qiao and co-workers created core–shell polymer dots on nanospheres by polymerizing carbon tetrachloride and ethylenediamine trapped in nanoparticles. Their study utilized a novel approach called "ship-in-a-bottle" to confine functional polymer chains in hollow nanospheres. Using this approach, they developed functional PCDs in hollow silica nanospheres and hollow carbon nanospheres. In addition to the feasibility of the isolation process, these core–shell structures could serve as carriers for different cargos, such as fluorescent imaging molecules and drugs.[78]



Fig. 2  Illustration of three different types of carbon dots (CDs), from left to right: carbon nanodots (CNDs), graphene quantum dots (GQDs) and polymer dots (PDs).

Zhu *et al.* utilized a moderate hydrothermal treating methodology to transform linear, non-conjugated polyvinyl alcohol (PVA) into fluorescent PCDs. According to this report, partially carbonized PCDs maintains the PVA chain structure, while their single PL excited state was demonstrated *via* ultrafast spectroscopy. The pH-dependent PL behaviour and bright fluorescence quality of PCDs, in the presence of polymers, such as chitosan-based hydrogels, PVA and so forth, make them an excellent candidates for bioimaging.[79,105,106]

# 3. Strategies of carbon dots synthesis

Based on the source of the substrate and the reaction method, the basic synthetic techniques for preparing CDs are conceptually categorised into "top-down"[31,107] and "bottom-up"[108] approaches.

## 3.1. Bottom-up approach

One of the most effective ways to produce fluorescent CDs on a large scale is the "bottom-up" approach, schematically depicted in Fig. 3. In general, bottom-up methods applied organic molecules or macromolecules as the precursors for the fabrication of CDs. This methodology has gained considerable popularity in recent years due to its operational simplicity, controllable reaction conditions, the possibility of using inexpensive raw materials, and the feasibility of a one-step high-volume CDs synthesis.[70,109–111]

Various reports have confirmed the bottom-up synthesis of CDs using small organic molecules as the precursor *via* combustion, plasma, and thermal synthesis approach.[112–114] In these processes, the small molecule precursors undergo multiple critical steps, including dehydration, condensation, polymerization, and further carbonization and modification.[70]

Several precursors have been used as the starting component for creating CDs *via* the bottom-up approach, including organic salts, such as octadecylammonium citrate or diethylene glycol ammonium citrate,[115] coffee grounds,[116] glycerol,[116] L-glutamic acid,[117] ascorbic acid,[118] citric acid,[8,119] and ethylenediaminetetraacetic acid disodium salt.[120] Since the CDs' structure, surface-functionalization, and photoluminescence are directly associated with the precursors and the synthesis procedures, the selections of suitable starting materials and sets of optimized conditions are fundamental steps in CDs manufacturing *via* bottom-up methods. For instance, similar CDs made with the same synthesis method, but using different precursors, can lead to different behaviours and hence different applications.[121–123]

The bottom-up methods typically require elevated reaction temperatures, high-grade carbon precursors, toxic organic solvents, and alkaline/acid treatments. Yet, the beneficial effects of controllable size and optimisable synthetic conditions outweigh their harsh synthesis conditions.[124] Highly adaptable bottom-up strategies lead to endless possibilities for concurrently tuning the properties of CDs and their applications.[125] However, it should be noted that applying high temperature and harsh reaction conditions to the organic molecules lead to condensation, nucleation, and subsequent formation of highly polydispersed CDs, which might not be suitable for specific applications.
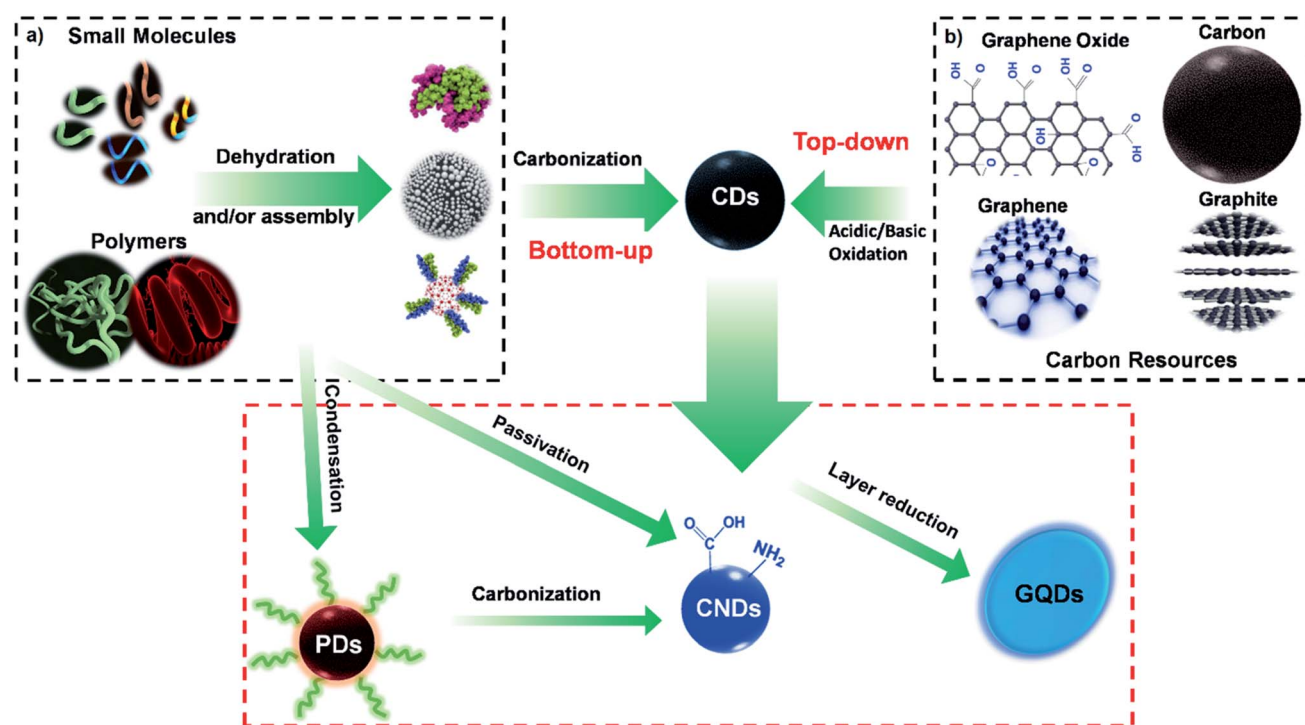


Fig. 3 Schematic illustration of the production routes of CDs: (a) "bottom–up" synthesis, where CDs are prepared from organic molecules or polymers through hydrothermal, calcination, microwave radiation, and not limited to these methods; (b) "top–down" synthesis, where CDs are prepared from larger sized carbon resources through acidic oxidation, hydrothermal cutting, and electrochemical methods.

The prevalent bottom-up approach includes microwave irradiation, hydrothermal/solvothermal treatment, and pyrolysis, which are briefly discussed in the following sections and some examples of their applications.

**3.1.1. Microwave irradiation.** Microwave irradiation is considered to be a rapid, convenient and inexpensive method in which the decomposition of chemical bonds, as well as carbonization of precursors, occur *via* the electromagnetic irradiation in the wavelength range from 1 mm to 1 m.[114,126,127] However, even a slight change of the reaction parameters, such as irradiation power and absorption properties of the precursors, could produce low-quality CDs with a high level of polydispersity and large average sizes.[128]

One of the most appealing attributes of this microwave irradiation for the synthesis of CDs is its very rapid reaction time. For instance, Liu and his colleagues used a disaccharide, such as sucrose, as the carbon source and diethylene glycol (DEG) as the reaction media to synthesise green luminescent CDs *via* microwave irradiation, within only one minute. The DEG-stabilized CDs (DEG-CDs) had an average size of about 5 nm, and could be well dispersed in an aqueous solution with a transparent appearance. The DEG-CDs displayed upconversion PL spectra and showed a fixed emission peak at 540 nm. This emission peak did not shift as the excitation wavelength was altered from 320 to 380 nm, confirming that the emission was recorded from the lowest single state without being affected by excitation mode. The highest upconversion PL was obtained at the excitation wavelength of 740 nm. These upconversion PL properties provided an efficient system to be incorporated into the C6 glioma cells with low cytotoxicity, presenting their potential for bioimaging applications.[113]

In another example, Zhai *et al.* investigated the microwave-mediated synthesis of CDs from citric acid and a number of amine molecules to produce highly luminescent CDs. The amine molecules, especially the primary amines, displayed a dual function as N-doping starting materials and surface passivating agents for the CDs, which improved the PL performance. The quantum yield values significantly increased by increasing the N content of the CDs synthesised from citric acid and 1,2-ethylenediamine, reaching 30.2%. The resultant CDs were highly biocompatible and exhibited a high potential for biomedical applications.[114]

**3.1.2. Hydrothermal/solvothermal treatment.** The hydrothermal treatment is arguably one of the unique techniques used to fabricate new carbon-based nanomaterials due to its low cost, non-toxicity and environmentally friendly features.[53] Typically, a solution of organic precursors is sealed in a hydrothermal reactor at a high temperature.[129] Using hydrothermal carbonization (HTC), CDs can be produced from various organic materials, including cysteine (cys) and citric acid,[130] glucose,[131] food waste,[40] chitosan,[132,133] banana extract[134,135] and many other natural polymers.[128]

The CDs synthesised *via* the hydrothermal method possessed remarkable optical properties, and the post-treatment reactions in most cases are plain. Mohapatra *et al.* synthesised highly photoluminescent CDs by HTC of orange juice, resulting in a QY (quantum yield) of 26%.[92] These "semiconductor quantum dots'' (1.5–4.5 nm in size) were used in bioimaging because of their low toxicity and high photostability. Liu *et al.* considered a one-step process for fabrication of amino-functionalized fluorescent CDs by HTC of chitosan at 180 °C for 12 h.[136]

Solvothermal carbonization, followed by organic solvent extraction, is another commonly used technique for synthesizing CDs.[45,136] In this method, carbon-yielding compounds are heated in high boiling point organic solvents, such as ethanol, dimethylformamide (DMF), glycol, and formamide, followed by extraction and purification procedures. Bhunia *et al.* produced hydrophilic and hydrophobic CDs from carbohydrate carbonization with diameters of less than 10 nm.[136]

The hydrophobic CDs were produced by mixing various amounts of carbohydrates, octadecylamine, and octadecene, followed by heating to 70–300 °C for 10–30 min. The hydrophilic CDs could be produced by heating the aqueous solution of carbohydrates at various pHs. The hydrophilic CDs with red and yellow emissions could be developed by mixing an aqueous solution of carbohydrates with concentrated phosphoric acid, then heating to 80–90 °C for 60 min.

**3.1.3. Pyrolytic process.** The pyrolytic reaction typically occurs under high endothermic heat, controllable pressure, and an inert atmosphere in the presence of a high concentration of acid and alkali solutions. Under the pyrolytic conditions, the chemical bonds in the organic molecule precursors undergo a series of decomposition processes, cleaving the carbon substrate into a nanoparticle. The physicochemical properties of the synthesised CDs can be modulated by changing the reaction conditions of pyrolysis, for instance, its temperature, pH value and duration of the process.[137]

Due to its ease of use, scalability, rate of production, and low cost, pyrolytic reactions are prevalent for the production of carbon dots.[138,139] For instance, Feng *et al.* employed a facile pyrolytic method to develop carbon dots from readily available D-glucose and L-aspartic acid as the precursors. In their process, the solution of starting precursors in aqueous NaOH was subjected to 200 °C for 20 min. The obtained CDs were about 2.28 ± 0.42 nm in diameter. The prepared CDs displayed optimal biodegradability and adjustable colour emission properties that could be used for labelling C6 glioma cells in the absence of targeting molecules. Their results also confirmed that the CDs could pass through the blood–brain barrier and accurately target the malignant tissue.[140]

### 3.2. Top-down approach

Unlike the bottom-up approach, where CDs are produced from smaller molecules, larger sized carbon sources are used to create smaller CDs in the top-down approach (Fig. 2b). In the top-down approach, the CDs are obtained by oxide cutting carbon resources, such as graphite powder,[141] carbon rods,[142] carbon fibres,[143] carbon nanotubes,[7,144] carbon black,[145] graphene oxide (GO),[146] activated carbon,[141] and even candle soot.[147]

The oxide cutting methods used for downsizing the carbon resources, which create CDs, inevitably leave behind negatively charged oxygenated groups on the resultant carbon dots, creating a hydrophilic and defective surface in the graphitic structure. One

of the most challenging issues with these methods is the difficulty in thoroughly eliminating the excess amount of oxidizing agent. Therefore, other top-down cutting routes with more controllable parameters are used, including electrochemistry,[148,149] hydrothermal or solvothermal methods,[150,151] metal–graphite intercalation,[152] and strong physical etching. The strong physical etching consists of arc discharge,[153] laser ablation,[154] and nanolithography by reactive ion etching.[155,156]

In the electrochemistry method, CDs have been synthesised by electrochemical cleavage of carbon-based electrodes such as carbon nanotubes (CNTs),[157] graphite rods,[142] reduced graphene oxide (rGO) film[158] and three-dimensional chemical vapour deposited grown graphene.[159] The electrolytes used in the electrochemical top-down approaches include ethanol,[142] ionic liquids,[148] $NaH_2PO_4$,[160] tetrabutylammonium perchlorate (TBAP),[161] and phosphate-buffered saline (PBS)/water.[158,162]

The electric field applied to the electrodes peels off nanosized carbon fragments from the electrode surface *via* graphite layer intercalation and radical reactions.[163] To enhance the efficiency of the electrochemical method, some studies have used ionic liquids to aid with the electrochemical exfoliation of graphite electrodes. In this approach, the ionic liquid solvent can improve the reaction significantly, as the ionic solution can dissolve and catalyse simultaneously. Moreover, by changing the ratio of the ionic liquid and water, the fluorescence emission wavelengths of the resulting CDs could be tuned.[148,164] However, this method does not provide high fluorescence quantum yield and further optimization steps are required.[165]

In the following sections, the early preparation methods of CDs production by top-down approach are discussed.

### 3.3. Chemical ablation

Chemical ablation is a method where strong oxidizing acids carbonize organic molecules to carbonaceous particles, which can be further cut into smaller sheets by controlled oxidation.[166,167] Peng and Travas-Sejdic studied an easy route for synthesising luminescent CDs in an aqueous solution by dehydrating carbohydrates with concentrated sulfuric acid. They then divided the resulting carbonaceous materials into individual CDs using nitric acid, and eventually passivating the particles with amine-terminated compounds, such as 4,7,10-trioxa-1,13-tridecanediamine. It was found that the critical step for the PL properties of these CDs was surface passivation. In addition, the CDs emission wavelength could be adjusted by varying the number of treatments with nitric acid and the starting material. The multicolour emission and non-toxic nature of the CDs prepared by this approach made them suitable for biomedical applications.[168]

### 3.4. Electrochemical carbonization

Electrochemical carbonization is a technique for synthesising CDs without heat treatment using several bulk carbon materials as the carbonous precursor.[169–172] Unlike the more recent electrochemistry methods in which the carbon-based electrodes are used as the source of carbon for the synthesis of CDs, the solution is converted to CDs in electrochemical carbonisation.

For instance, Zhang *et al.* presented the synthesis of CDs through electrochemical carbonisation of low-molecular-weight alcohols.[173] They used two platinum (Pt) sheets as the supplementary and working electrodes and a reference calomel electrode mounted on a freely adjustable lugging capillary. In this process, the alcohol is transformed into CDs after electrochemical carbonisation. The size and graphitization degree of CDs obtained by this method increasing with increasing the applied potential. The resulting CDs had an amorphous core with brilliant excitation and size-dependent PL characteristics without complicated purification and passivation procedures. The QY of these CDs could reach up to 15.9%.[169]

### 3.5. Laser ablation

Laser ablation (photoablation) is when high fluence, short-wavelength laser radiation interacts with attenuating materials.[174] Sun *et al.* utilized a Q-switched Nd:YAG laser (10 Hz, 1064 nm) ablation, from which the carbon target, a mixture of graphite powder and cement under heat processing, was in a flow of argon gas carrying water vapour (*via* a water bubbler) at 900 °C and 75 kPa.[175] To reach a bright luminescence emission, the resulting CDs were refluxed in nitric acid for 12 h, and their surface was passivated by attaching simple organic molecules, such as amine-terminated polyethylene glycol and poly(propionyl ethyleneimine–ethyleneimine).[176,177] Du *et al.* reported the fabrication of fluorescent CDs by laser irradiation of citric acid in the presence of 1,2-ethylenediamin.[178] They evaluated the sensing application of the CD quenched with $Hg^{2+}$ for iodide detection based on the competitive binding mechanism either in aqueous media or in human urine samples.

The emitted luminescence was influenced by the state of ligands localised on the CDs' surface. Therefore, the surface characteristics of CDs could be tuned to reach the desired light emission properties. In another example, Li *et al.* used laser ablation to synthesise CDs from nano-carbon materials as the precursor dispersed in a solvent such as acetone, ethanol, or water.[80] First, a dispersion of 0.02 g of Sigma-Aldrich nano-carbon precursor in 50 mL of solvent (ethanol, acetone, or water) was prepared. After ultrasonication, 4 mL of suspension was dropped into a glass cell covered by a quartz window, and light at a wavelength of 532 nm was applied under mild magnetic rotation.

Because of this fabrication method, the CDs had a core–shell structure, with an amorphous outer layer and an onion-like carbonous inner structure with a hollow centre. It was demonstrated that the origin of the PL intensity was laser irradiation of the carbon substrate, which led to different oxygen groups on the surface of the CDs. The number of oxygen groups on the surface was tunable and increased by enhancing the irradiation energy and irradiation time.

To summarize, the characteristics of various synthesis methods for the preparation of CDs are presented in Table 2. As listed in Table 2, each strategy has particular advantages and disadvantages. In general, poor control oversize is a common concern in most synthesis procedures. On the other hand, most methods are cost-effective, among which the hydrothermal approach provides higher QY values.

Table 2 Different methods for the synthesis of CDs with their specific advantages and disadvantages. BU and TD are abbreviations for bottom-up and top-down approaches, respectively, and QY is the quantum yield

| Synthesis methods | Approach | QY (%) | Advantage | Disadvantage | Reference |
|---|---|---|---|---|---|
| Chemical ablation | BU | 4.34–28 | Wide range of starting materials, most accessible method | Drastic and harsh processing conditions, multiple steps, poor control oversize | 141, 143, 150, 168 and 179–184 |
| Hydrothermal/ solvothermal treatment | BU | 1.1–94.5 | Cost-effective, eco-friendly, non-toxic | Poor control over size, low production yield | 133 and 185–191 |
| Solid-state thermal treatment | BU and TD | 9–69 | Cost-effective, eco-friendly, non-toxic | Poor control oversize | 192–197 |
| Electrochemical carbonization | TD | 15.9–46.2 | Cost-effective, high QY, reasonable control over fabrication parameters | Limited small-molecule precursors, relatively low QY | 144, 161, 162, 198–202 |
| Microwave irradiation | BU | 2–44.9 | Rapid process, cost-effective, eco-friendly | Poor control oversize | 113, 114, 127, 178 and 203–208 |
| Laser ablation | TD | 4–36 | Tunable surface states, rapid process, effective, high production yield | Poor control over size, low QY | 209–213 |

The main challenges associated with the fabrication of CDs include: (a) carbonaceous aggregation during carbonization, which can be bypassed by utilizing electrochemical synthesis, solution chemistry, or confined pyrolysis methods; (b) broad size distribution tampering the optical properties, which can be further optimized through post-treatment involving centrifugation, gel electrophoresis, and dialysis; (c) controlling surface characteristics that are crucial for solubility, which can be tuned during synthesis or post-treatment.

For most conventional synthesis methods of CDs, exerting complete control over the size distribution, PL intensity, and other essential characteristics of CDs have remained challenging. Therefore, developing novel fabrication methods with more flexible and tunable reaction conditions is highly sought after.

One example of such a synthesis technique is the non-thermal microplasma process. Non-thermal microplasma is a promising technology for nanomaterial synthesis and treatment, which offers favourable features, such as low cost, high purity, controllable size, and mild synthesis conditions, including moderate reaction temperatures and pressure, low toxicity limited modification steps.[214,215] Therefore, this approach could address the non-uniform size distribution of CDs that occurs in multiple conventional fabrication methods, such as hydrothermal treatment.[216]

High-energy electrons are produced from the non-equilibrium plasma generate active species, leading to rapid chemical reactions under mild conditions (e.g., atmospheric pressure and low temperature).[217,218] In one study conducted by Ma et al., the synthesis of luminescent carbon quantum dots was performed by an in-house-designed plasma reactor where isopropanol was utilized as the only substrate in the reaction without any need for acid/base or metal ions. The resulting CDs demonstrated a narrow average size of about 1.78 nm and excitation-dependent emission spectra within the 310–410 nm excitation wavelengths. Additionally, functional groups such as C=O and OH were found to attach to the surface of CDs during the plasma reaction.[72]

In another study by the same group, the same technique was exploited to dope the CDs with functional nitrogen groups, including NH, to achieve pyrrolic-like structures. These N-doped CDs had an average size of 5.98 nm and a QY of up to 9.9%. The results further revealed that both plasma treatment time and operating voltage have a direct impact on the carbonization degree, particle size distribution and different PL intensities.[216]

## 4. Photoluminescence mechanisms in CDs

The synthesis route undertaken to produce CDs will directly impact their fluorescence properties. Therefore, optimising and controlling the synthesis method of CDs is the key factor in engineering CDs optical properties suitable for the desired application. The link between the synthesis methods and CDs photoluminescence, however, is mostly neglected. In this regard, it is essential first to understand the origin of photoluminescence in CDs. Some of the photoluminescence mechanisms proposed for fluorescent nanodots have been suggested for CDs as well.[45,219,220] Fig. 4 shows the three major photoluminescence mechanisms for nanodots, indicating their specific features.

The dominant PL mechanism in "pure" quantum dots belongs to the radiative band-edge recombination. This PL is commonly named the intrinsic interband transition or band-edge electron–hole recombination. Upon the absorption of a photon with energies superior to the bandgap energy ($E_g$), an electron from the valence band is raised to the conduction band, leaving a hole behind. Following the recombination of the excited electron back to lower valence bands, a photon of light is emitted (Fig. 4a). This has a lower emission wavelength due to the energy lost in a non-radiative decay to the bottom of the conduction band before the electron–hole recombination process.

This PL mechanism is only valid in defect-free and impurity-free quantum dots, where no interstates within the bandgap
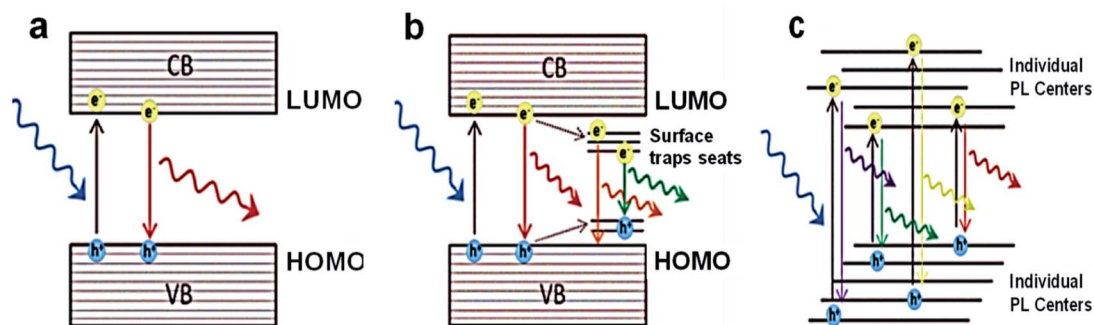
Fig. 4 Scheme of the various photoluminescence mechanisms and their unique characteristics: (a) SQDs with quantum confinement, where the size-dependent PL, excitation-independent PL has narrow PL band and long lifetimes; (b) CDs/GQDs with quantum confinement, where the size-dependent and excitation-independent PL has a broad PL band and medium lifetimes; (c) CNDs with no quantum confinement, where the size-independent and excitation-dependent PL has a broad PL band and short lifetimes.[49] Adapted from ref. 49 with permission from the Royal Society of Chemistry (Great Britain), copyright 2021.

exist. In this perfect scenario, quantum confinement entirely controls the PL properties. The PL emission band is also very narrow (FWHM to 40 nm) and independent of the excitation. The latter attribute of this PL mechanism suggests that as long as the excitation exhibits a higher energy than the bandgap, the PL emission has a maximum at a fixed position irrespective of the excitation wavelength used, since the emission wavelength is always the same, i.e., equal to the bandgap. Although this mechanism is valid for ideal nanodots, it can be applied to the semiconductor quantum dots (SQDs).

A more realistic PL mechanism can be proposed when trap states are present in the bandgap because of impurities, surface defects, functional groups, and adsorbed molecules. In these cases, the photoexcited electron and/or hole can be trapped, and their subsequent recombination leads to a radiative emission of lower energy (Fig. 4b). Consequently, the observed PL response is categorized with at least two mechanisms from different sources as below:

(1) Core with its intrinsic quantization effects.

(2) Particle surface properties are governed by the surface functional groups and surface defects (referred to as surface trapping states) (Fig. 4b).

Most of the CDs and GQDs follow this type of PL response. Both kinds of carbon-based nanodots have the shared characteristics of presenting excitation-dependent emission, given a reduction in the emission signal systematically displaced to longer wavelengths as $\lambda_{ex}$ increases.[220]

An example of the PL mechanism of GQDs is the PL behaviour of the chemically derived GO, which is explained first because GO is a significant raw material for GQDs preparation. Thus, GO and GQDs have similar chemical structures. GO comprises oxygen-based functional groups, either on the basal plane or at the edges. Hence, the 2–3 nm linearly aligned epoxy surrounds the aromatic $sp^2$ domains and hydroxyl-boned $sp^3$ C–O matrix.[160,161] The fluorescent properties are specified by the $\pi$ states of the $sp^2$ sites because GO has such a structure. The $\pi$ and $\pi^*$ electronic levels of the $sp^2$ clusters, which are influenced by the bandgap of the $\sigma$ and $\sigma^*$ states of the $sp^3$ matrix, are strongly

confined. Fluorescence can be facilitated by radiative recombination of electron–hole (e–h) pairs in such $sp^2$ clusters.[158]

The band gaps of different sizes of $sp^2$ cover a wide range, leading to a broad PL emission spectrum from the visible to near-infrared region because of the existence of broad size distribution of $sp^2$ domains in GO (Fig. 5).

The third primary type of PL results from the superposition of responses of assembled individual emitters (Fig. 4c). In such manners, neither quantum confinement nor a cumulative excitonic effect exists; therefore, the fluorescence behaviour is more related to that observed in metal nanoclusters.[219] The CNDs, which are achieved via bottom-up way at low temperatures, emit via this mechanism and produce a broad emission band due to the superposition of several emissions (i.e., various emitter centres). Moreover, when the surface emitter groups are quenched, this kind of PL is wholly suppressed via heavy atoms.

Recently, it has been reported that the carbogenic core starts forming at high temperatures and leads to PL because of the presence of both molecular fluorophores and the carbogenic core.[220] In this way, the result of the synthesis will be a combination of CDs and CNDs. It is possible to acquire most or exclusively CDs at higher temperatures.[16] The observed PL comes only from surface trap states that act as PL emitter centers in the absence of a carbogenic core formation.

Even when there is a very strong absorbance in the UV range, the absence of a comparable level of absorbance at the maximum excitation wavelengths together with the lack of fluorescence emission excited at the maximum of the UV excitation band support the idea that these fluorescent species consist of several individual emitters without a collective effect. There is no strong correlation between the position of spectral bands and particle size because of the absence of cumulative effects in the emission of CNDs. The spectral differences are then connected to different compositions of the particle surfaces.

Additionally, in contradiction to SQDs, in which the PL originates from intrinsic HOMO–LUMO transitions, the PL behaviour of CDs is roughly related to the synthetic methods,
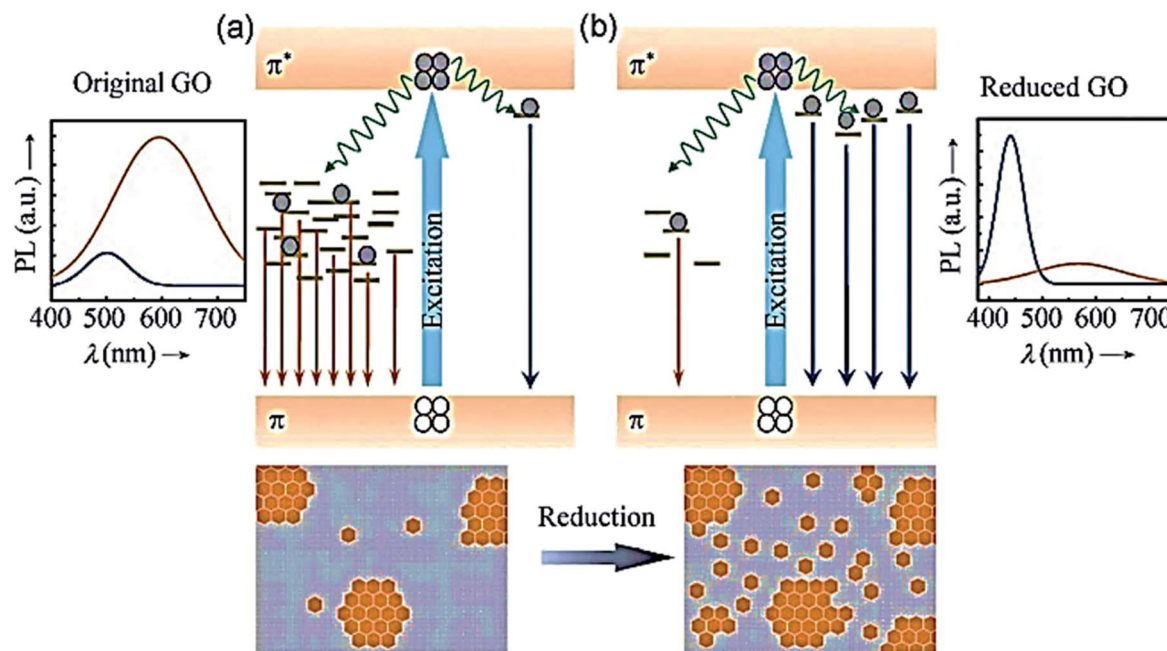
**Fig. 5** Proposed PL emission mechanisms of (a) the predominant "red emission" in GO from disorder–induced localized states and (b) the predominant "blue emission" in reduced GO from confined cluster states.[221] Adapted from ref. 221 with permission from John Wiley and Sons, copyright 2021.

conditions utilized for their synthesis, and subsequent passivation or functionalization strategies to modify their surface chemistry. Based on these factors, the competition between both the trap state emission and intrinsic state emission will change. Therefore, the PL origin will be the second or third type based on the prior classification.

Three factors are hypothesized to elaborate the emission of CDs: size dependency, a surface condition that generates luminescence, and implanted luminophores.[222] In terms of size dependency, various findings confirm that CDs have similarities with traditional QDs in size-dependent quantum confinement effect, creating the luminescence emission of CDs.[223,224] Yuan *et al.* fabricated nitrogen-doped surface decorated crystalline CDs synthesised precisely by bottom-up solvothermal method, evaluating the size distribution through TEM and AFM. They reported that the nanoparticle size increased from 1.95 nm (blue CDs) to 6.68 nm (red CDs) corresponding to the redshift. They attributed this alteration to the quantum confinement effect.[225] Although some studies revealed the same size-dependent mechanism, there is still a debate in accepting a correlation between the size and emission wavelength of CDs.[226,227]

The surface state is considered another influential factor in the PL mechanism since different engraftments have diverse energy levels.[29,227] Ding and his research group utilized a one-pot hydrothermal strategy for CD synthesizing. The amalgam CDs were afterwards followed by chromatographic separation. Their results demonstrated that luminescent CDs fractions were applied to the whole visible wavelength.[228] Furthermore, an increase in the presence of some functional groups (like carboxyl) and degree of oxidation led to a shift in the CDs emission as the lowest unoccupied molecular orbital (LUMO),

which is caused by oxygen components. They stated that the bandgap between the highest and lowest unoccupied molecular orbital decreased, and the amplifying surface oxidation of manufactured CDs resulted in a red shift in PL emission.

Molecular luminophores are another relevant element in CDs' PL emission, which are prepared *via* the bottom-up approach.[229–231] Zhang and co-workers reported that the hydrogen bonds between CDs and different polarized solvents could be a potential reason behind the shift in the red emission of their samples. Owing to the chemical composition and polarization of the solvent, the CDs emission was modified from 540 nm to 614 nm (green to red). Their results revealed that the hydrogen bond accounted for the major mechanism for the observed shift in spectrum.[232] From this point of view, it could be concluded that the fluorescent molecules generated through this manufacturing process showed high quantum yields,[233] because such purification process, which is therefore essential, removes other emission contributions.

## 5. Biomedical applications

Similar to inorganic fluorescent semiconductor nanoparticles (quantum dots) with tunable fluorescence emission, CDs can also emit light in different colours due to their quantum confinement, enabling size-dependent photon emission. Such optical diversity can undoubtedly be a critical driving force in the potential application of CDs in biomedical, electro-optical and photonic (optronics), catalysis, and sensing (Fig. 6). Since the use of CDs in optronics and catalysis has been widely reviewed,[234–236] the biomedical applications of CDs with an emphasis on sensing are discussed in this section.

**Biomedical**
- Biomedicine delivery system
- Bioimaging
- Biosensing and monitoring

**Chemical**
- Chemo-sensing

**Optronics**
- Dye-sensitized solar cells (DSCs)
- Organic solar cells (OSCs)
- Supercapacitor
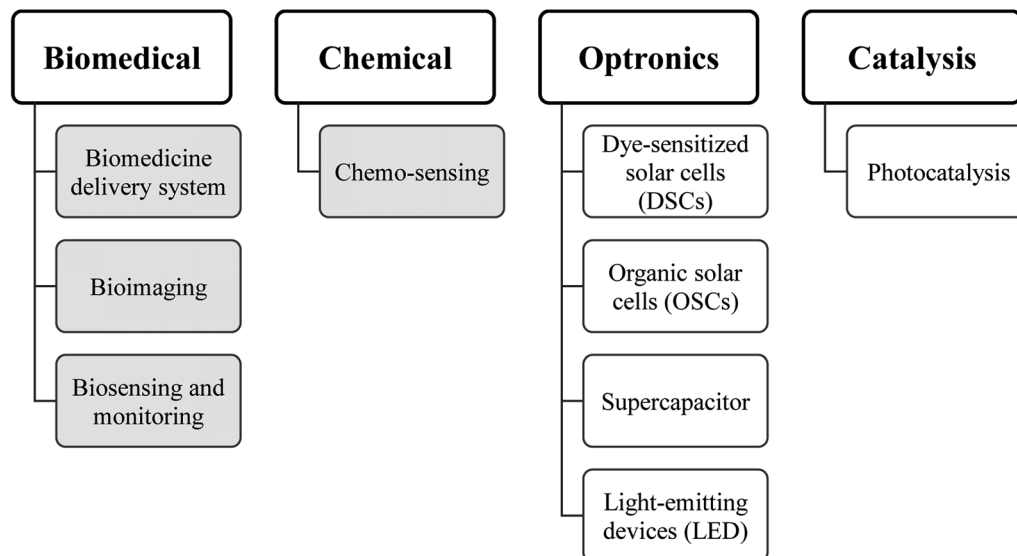- Light-emitting devices (LED)

**Catalysis**
- Photocatalysis

**Fig. 6** Classifications of potential applications of CDs.

Since CDs can be synthesised from natural carbon sources, they are generally more biocompatible and less toxic than inorganic quantum dots. CDs also bear active functional groups on their surface, which allow for further chemical modification. The combination of these factors and their unique fluorescence properties have led to mounting interest in their potential use for various medical applications, including biomedicine, bioimaging, biosensing, and therapeutics.

### 5.1. Biomedicine

Multiple studies have considered the therapeutic potential of CDs for certain diseases. S. Shankar *et al.* found that green-luminescent CDs prepared from styrene soot had an intriguing anti-angiogenic effect. The addition of CDs significantly reduced angiogenesis in an *in vitro* assay (Fig. 7).[237] Angiogenesis is the physiological process related to many tumours. Cancer cells make the proliferation of blood vessels around the tumour, thus preparing the needed nutrients for rapid multiplication of the cells and tumour growth. Indeed, a promising route in anticancer drug development is blocking angiogenesis. Even though the suitable mechanism for angiogenesis inhibition by the CDs has not been determined, scientists have found that the addition of the CDs resulted in lower expression of cellular growth factors known to promote blood vessel growth.

Haemostasis studies were carried out by Zhao *et al.* in 2017, where they synthesised carbon dots (CDs) by the utilization of egg yolk oil (EYO), known as the traditional medicine in China, first introduced for burn treatment, as well as acute and chronic eczema cases.[238] Their study showed that the biocompatible nature of the CDs has a significant impact on limiting the bleeding time, and stimulation and activation of coagulation and the fibrinogen system.[239] This finding agreed with other studies that used another Chinese traditional therapeutic agent, Schizonepetae Herba, on the haemostasis study.[240]
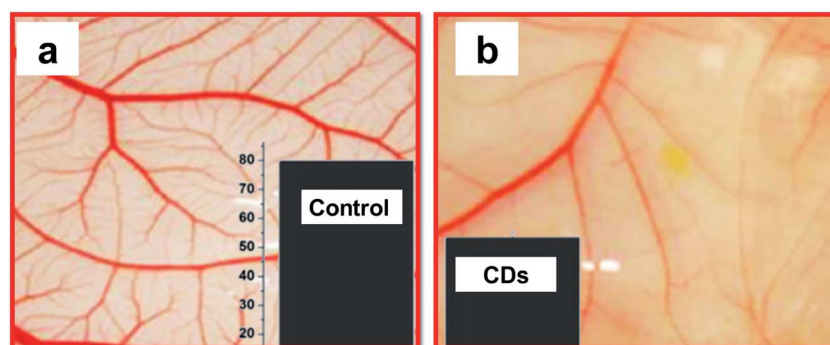
**Fig. 7** Anti-angiogenic effect of CDs. (a) Vascular density observed in buffer (recorded for chick embryos in a chick chorioallantoic membrane (CAM) assay); (b) much lower vascular proliferation upon treatment with CDs. Insets show a graphical representation of the haemoglobin level in the control and sample treated with CDs, adopted and modified from ref. 237. These images were adapted with permission from ref. 237. American Chemical Society, Copyright 2015.

In another study by Xu *et al.*, distinguished CDs with sp$^2$/sp$^3$ carbon and oxygen/nitrogen-based groups were synthesised by hydrothermal approach. The CDs demonstrated an acceptable efficiency for targeting anaemia without any side effects on the tumour cell proliferation. Further investigation of the impact of CDs on the cell cycle and its progression confirmed that CDs enhanced the crucial stage of humans RBC generation and erythroblast enucleation, without any adverse effect on the erythroid progenitor development and differentiation of the terminal erythroid.[241] Xia and his co-workers fabricated CDs from red beans and investigated the anti-proliferative effect of CDs on different cancer cell lines (*i.e.*, liver, pancreatic, colorectal adecnocarcinoma). According to their result, CDs decreased the cell migration significantly in all evaluated cancerous cell lines. Moreover, the major inhibition was reported in all cancer cell lines in the synarchism with doxorubicin. Therefore, they concluded that CDs could be an alternative and complementary medicine for cancer therapy.[242]

The combination of biocompatibility of CDs and the wide variety of surface functionalization pathways have unlocked new gateways for gene delivery applications. Liu *et al.* used a positively charged polymer, polyethyleneimine (PEI), as the starting material for preparing a PCD-based gene delivery platform.[76] In this approach, the hydrothermal method used to prepare PCDs led to the formation of the graphitic core CDs. As expected, the surfaces of the CDs displayed the cationic functional units of the starting PEI reagent (Fig. 8a). CD/pDNA gene delivery systems made from these CDs were illustrated using transmission electron microscopy, indicating that the DNA condensed on CDs formed larger nanoparticles with diameters less than 50 nm. This size range makes the CD/pDNA system favourable for an efficient cellular gene delivery (Fig. 8b).

Porphyra polysaccharide was introduced by Chen *et al.* as the carbon source for the one-pot hydrothermal approach. In this study, ethylenediamine (Ed) was decorated on the surface of the CDs for targeted delivery of multifunctional CDs. Their finding exhibited a higher rate of transfection efficacy than PEI and Lipofectamine2000. Investigating the cellular uptake mechanism determined that caveolae- and clathrin-mediated endocytosis is the primary route for nanoparticle internalization. Efficient gene delivery of the combinational gene based cargoes (Ascl1 and Brn2) resulted in the successful differentiation of ectodermal mesenchymal stem cells to neurons.[243]

In another study by Zhang *et al.*, functionalized CDs were prepared from hyaluronate and PEI *via* a bottom-up approach, and used for tumour targeting and gene delivery. It was found that the presence of charged polymer chains in the structure of the CDs mediated endocytosis, and further cellular uptake and transfection of CDs. The CDs also possessed an excellent condensation capacity, along with remarkable protective potential preventing nuclease degradation.[244]

A pseudohomogeneous carrier was first designed based on the chitosan precursor, which is decorated by arginine moieties. The result of the study showed that in addition to the noncytotoxic nature of the synthesised CDs, the vehicle could protect CDs from enzymatic degradation. The transfection efficacy was also much higher than blank chitosan and even PEI as the favourable control polymer. They concluded that arginine engraftment acts as a CPP, and enhances cellular internalization and consequent transfection.[245]

In addition to DNA delivery by linking the DNA cargo to the CDs through electrostatic attraction, a number of research studies have demonstrated that the direct synthesis of CDs from oligonucleotides as the carbon source and subsequent cell uptake of the CDs. H. Ding *et al.* fabricated DNA-extracted CDs and proved that they could be readily internalized into cells.[246] Fig. 9 shows the method wherein purified natural DNA was hydrothermally treated, yielding fluorescent CDs.

CDs are effective delivery vehicles since they overcome some of the obstacles that other conventional delivery carriers cannot address, such as monitoring and tracking the therapeutic agents in the malignancy site and quantifying the biological response to therapy. Therefore, thanks to their tunable surface charge and modifiable functional groups, CDs are exploited for more efficient cargo delivery systems.[165]

Wang *et al.* synthesised a nanocomplex of DOX/CD by a hydrothermal oxidation method to facilitate drug therapy *via* image guidance. They used citric acid and *o*-phenylenediamine
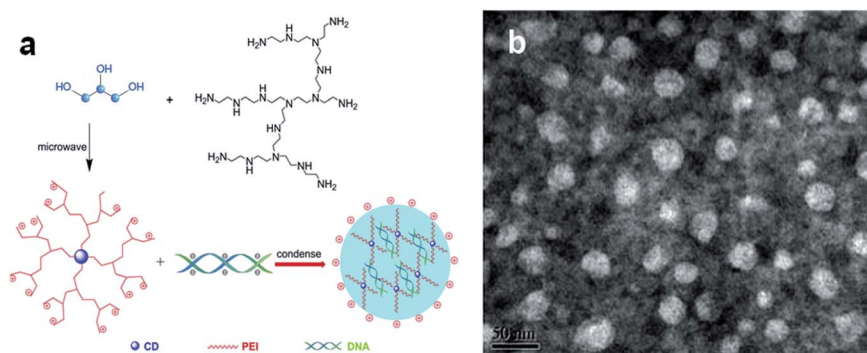


**Fig. 8** The scheme depicts the preparation of a gene delivery platform using CDs as vehicles. (a) The CDs are prepared through microwave-induced hydrothermal treatment of glycerol and polyethyleneimine. The CDs were incubated with DNA, forming the transfection agent following further condensation; (b) TEM images of negatively stained CDs/pDNA complexes. They were adopted and modified from.[76] These images were adapted with permission from ref. 76. Elsevier, copyright 2021.
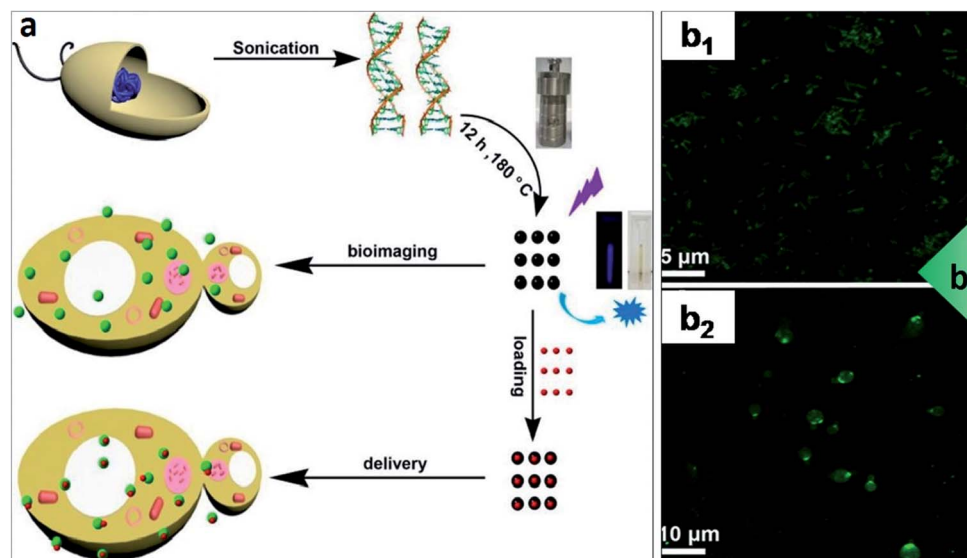
**Fig. 9** CDs synthesised from oligonucleotides precursor as a cellular delivery vehicle. (a) The scheme depicts the hydrothermal synthesis of CDs from purified DNA and employing the CDs for either bioimaging (making use of their fluorescence) or delivery into cells (upon attachment of molecular cargo onto the CDs); (b) DNA–CDs were readily internalized by bacteria and yeast. DNA–CDs entered (b1) *E. coli* or (b2) *S. cerevisiae* cells and emitted green signals upon UV irradiation (405 nm) as shown on CFM images.[246] These images were adapted with permission from ref. 246. American Chemical Society, Copyright 2015.

as carbon sources for CD production, along with loading the nanoparticles with positively charged DOX through electrostatic interaction between DOX molecules and negatively charged functional groups on the surface of CDs. Their result confirmed that DOX/CDs induced selective toxicity toward the cancer cell lines, while remaining relatively passive for normal cells. In addition, DOX/CD exhibited a reversible donor-quenched mode dependent on the release of cargo. Briefly, conjugation of DOX with CDs turned the CDs signal off (*i.e.*, OFF mode), and after the drug was released *via* endocytosis cellular uptake process, the mode shifted to ON, and a signal was detectable through the emitted fluorescent light.[247]

Similarly, Kong and his colleagues developed DOX/CD as a drug carrier using citric acid and ethylenediamine as precursors to fabricate CDs *via* the hydrothermal procedure. Their results showed a relatively high DOX loading capacity for CDs, which could be efficiently utilized in cancer therapy. The DOX-conjugated CDs showed remarkable cellular internalization and anti-proliferative activity on MCF7 cell lines compared to free DOX, suggesting a good potency to serve as an option for cancer drug delivery application.[248]

In another study, Zheng *et al.* designed CDs to bypass oxaliplatin on the surface through functional amino groups. The fabricated CDs presented great potential for endocytic uptake into the hepatic cancerous cells. Because of the reducing environmental properties in cancer cells, oxaliplatin could be released from CDs into the cancer cells. In addition, CDs were used for image-guided drug delivery, revealing that intra-tumoral injection of fabricated CD reduced the volume of the tumour without any significant systematic toxicity.[249]

The fluorescent CDs for delivery of mitomycin manufactured by *Daucus carota* subsp. *Sativus* (carrot) is another example of

eco-friendly CDs application in drug delivery. The designed nanovehicle was faced with breaking hydrogen bonds in the lesion site (pH 6.8), so it makes them release the drug. In addition to the narrow size distribution and biocompatibility characteristics, this formulation guaranteed the high cellular uptake of myosin CDs by *Bacillus subtilis* cells. The *in vitro* study showed that the cargo was successfully loaded into the CDs structure with efficient cellular internalization. The pH-related release pattern and biocompatible nature of the synthesised CDs were also confirmed on MCF-7 cancer cells.[250]

Fahmi *et al.* exploited a biocompatible green approach for manufacturing bamboo leaf cellulose into CDs modified by 4-carboxy-benzyl boronic acid for targeted doxorubicin delivery to HeLa tumour cells. What distinguished their synthesised CDs was that, in addition to the non-toxicity and biocompatibility, they exhibited a high range of stability in variable pH range and at ion strength. The *in vitro* studies showed adequate folate receptor-mediated cellular uptake in HeLa cells.[251]

### 5.2. Bioimaging

CDs are conduits for biological imaging and have significant advantages compared to other quantum dots used for bio-imaging. Fig. 10a shows a typical colourful imaging application of CDs for cell imaging.

Using the optical properties of CDs, Nandi *et al.*[252] conducted cell labelling *via* amphiphilic CDs, where CDs were made from long hydrocarbon chains covalently joined to the graphitic cores. Lu *et al.* used CDs to label the HL-7702 cells, and indicate the absence and presence of copper ions for biosensing and imaging of $Cu^{2+}$ in liver cells (Fig. 10b).[253] The fabricated system exhibited excellent optical properties of dual-emission by single-wavelength excitation. In another study, mitochondria
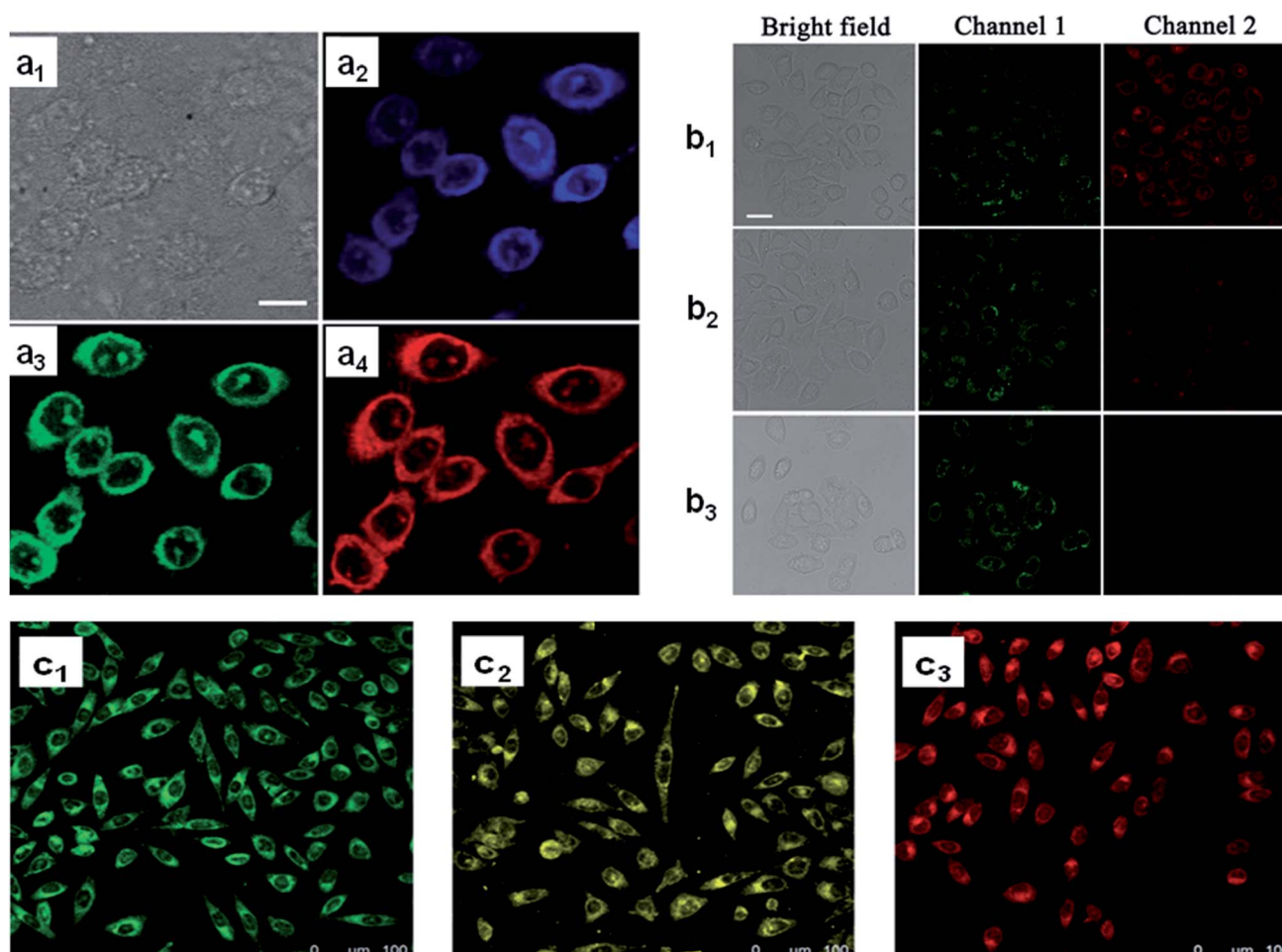
Fig. 10 Cell imaging using CDs. (a) Confocal fluorescence microscopy images of CHO cells incubated with amphiphilic CDs embedded within phospholipid small unilamellar vesicles, (a1) bright-field image, (a2) images recorded at an excitation of 405 nm and emission filter 525/30 nm, (a3) excitation of 488 nm and emission filter 525/30 nm, (a4) excitation at 561 nm and emission 641/40 nm. Scale bar is 10 μm;[252] (b) CLSM images of live HL-7702 cells using 0.1 mg mL$^{-1}$ CDs. (b1) Before and (b2 and b3) after treatment, (b2) with $10^{-6}$ M Cu$^{2+}$ and (b3) $10^{-5}$ M Cu$^{2+}$. Scale bar is 25 μm;[253] (c) confocal fluorescence microscopy images (excitation at 405 nm) of MCF-7 cells incubated with CDs prepared from (c1) meta-phenylenediamine, (c2) ortho phenylenediamine, and (c3) paraphenylenediamine. Each CDs label provides a distinct fluorescence emission peak (e.g., distinct colour).[256] These images were adapted with permission from ref. 252, 253 and 256. RSC, Elsevier and John Wiley and Sons. Copyright 2021.

served as a CD carrier for *in vivo* imaging and DOX delivery. After mitochondria isolation, the CD that contained DOX was loaded in the organelle's inner space, and applied as an imaging and therapeutic agent for cancer cells. With this technique, a great biodistribution of the drug and considerable preservation of optical properties were observed *in vivo*.[254]

Most CDs utilized in bioimaging applications and described here are water-soluble (hydrophilic), where the degree of CDs hydrophilicity can affect the cell uptake and degree of colouring.[255] In this regard, Jelinek *et al.* explored the impact of water solubility of CDs on their performance for bioimaging by using a range of precursors with varying levels of hydrophilicity (*meta*-phenylenediamine, ortho phenylenediamine, and para-phenylenediamine).[256] The confocal fluorescence microscopy images of epithelial cells incubated with these CDs endowed each CDs species with a different emission wavelength, as shown in Fig. 10c. It was found that the water-soluble CDs had

bright and monochromatic emissions. They were internalized by the cells, and mostly concentrated in the cytosol. By employing different excitation/emission wavelengths, distinctive features of the cells could be visualized based on the nature of the CDs used. Table 3 gives an overview of the CDs used in bioimaging and imaging, along with their synthesis and applied conditions.

Another aspect of using carbon dots in bioimaging is their implementation in photoacoustic imaging (PA) and photothermal therapy (PPT), which have grabbed extensive interest due to their non-invasiveness and insignificant tissue damage.[265,266] Feasible PTT and PA imaging agents should have high absorption coefficients, as well as photothermal conversions within 650–950 nm,[267,268] considered as the biological transparency window, and accumulation in the lesion site.[269]

Bao and his coworkers demonstrated that sulfur and nitrogen codoped near-infrared region (NIR) CDs were efficient

**Table 3** A representative overview of the selected CDs used in imaging and bioimaging along with their synthesis methods, characterization, and application

| Synthetic method | Precursor/reactants | QY (%) | Excitation range (nm) | Emission range (nm) | Max of em @ ex (nm) | Size (nm) | Application | Reference |
|---|---|---|---|---|---|---|---|---|
| Hydrothermal | Bagasse wastes | 12.3 | 330–510 | ~430–550 | $\lambda_{em,max} = 470$ @ $\lambda_{ex} = 390$ | 1.8 | Bio-imaging (cancer cell) | 36 |
| Ultrasound irradiation | Food wastes | 2.8 | 330–405 | ~410–470 | $\lambda_{em,max} = 410$ @ $\lambda_{ex} = 330$ | 4 | Bio-imaging (cancer cell) | 40 |
| Hydrothermal | Folic acid | 58.0 | 325–425 | ~440–460 | $\lambda_{em,max} = 445$ @ $\lambda_{ex} = 365$ | 3.5 ± 0.6 | Bio-imaging (cancer cell) | 257 |
| Hydrothermal | (1) 6-O-(O-O'-di-lauroyl-tartaryl)-D-glucose; (2) 6-O-(O-O'-di-lauroyl-tartaryl)-L-ascorbic acid; (3) Vitamin B1 + oleic acid | (1) 6.5 (2) 7.4 (3) 14.5 | (1) 350–500 (2) 350–550 (3) 350–600 | (1) 490–570 (2) 520–630 (3) 580–650 | (1) $\lambda_{em,max} = 525$ @ $\lambda_{ex} = 450$; (2) $\lambda_{em,max} = 560$ @ $\lambda_{ex} = 475$; (3) $\lambda_{em,max} = 585$ @ $\lambda_{ex} = 475$ | 4.2 ± 0.6 | Environmental (solid state lighting) | 257 |
| Laser ablation | (1) 1-n-Butyl-3-methylimidazolium tetrafluoroborate (BMI·BF$_4$); (2) 1-n-Butyl-3-methylimidazolium bis(trifluoromethanesulfonyl) imide (BMI·NTf$_2$); (3) 1-n-Octyl-3 methylimidazolium bis(trifluoromethanesulfonyl) imide (OMI·NTf$_2$) | (1) 5.0 (2) 19.0 (3) 20.0 | 340–520 | ~410–580 | $\lambda_{em,max} = 560$ @ $\lambda_{ex} = 520$ | 1.5, 2.9 and 3 | Ionic liquid | 211 |
| Hydrothermal | Poly(vinyl alcohol) (PVA) and ethylenediamine (EDA) | 35.0 | 240–400 | ~410–465 | $\lambda_{em,max} = 410$ @ $\lambda_{ex} = 340$ | — | Environmental (solid state lighting) | 258 |
| Hydrothermal | 4,7,10-Trioxa-1,13-tridecane diamine (TTDDA) and citric acid | 21.0 | 340–500 | ~430–525 | $\lambda_{em,max} = 430$ @ $\lambda_{ex} = 340$ | 4 | Bio-imaging (cancer cell) | 259 |
| Microwave | Latex | — | 460 | 360–520 | 360–520 | 2–8 | Metal sensing and cellular imaging | 260 |
| Hydrothermal | Citrate and urea | 93 | 400–525 | 535 | $\lambda_{em,max} = 535$ @ $\lambda_{ex} = 488$ | 2.75 | Bio-imaging (cancer cell) | 261 |
| Microwave | Tissue paper | — | 200 to 900 | 500 | $\lambda_{ex}/\lambda_{em} = 400/520$ | 4.2 | Determination of glutathione | 262 |
| Hydrothermal | Pear, avocado, kiwi, and citrate | 20–35 | 470 | 500 | $\lambda_{em,max} = 538 - 529 - 544 - 546$ (respectively) @ $\lambda_{ex} = 4870$ | 3.98–4.35 | Bio imaging | 263 |
| Hydrothermal | Linseed | 14.2 | 242-324 | 503 | $\lambda_{em,max} = 503$ @ $\lambda_{ex} = 395$ | 4–8 | Bio-imaging (cancer cell) | 264 |

Table 4  A representative overview of the selected studies of carbon-based nanomaterials including CDs and their applications in chemo-/bio-sensing

| Synthetic method | Precursor/reactants | Excitation range (nm) | Emission range (nm) | Max of em @ ex (nm) | Size (nm) | Sensing application | LOD | Linear range | Analyte | Reference |
|---|---|---|---|---|---|---|---|---|---|---|
| Hydrothermal | 4,7,10-Trioxa-1, TTDDA& citric acid | 340–500 | ~430–525 | $\lambda_{em,max} = 430$ @ $\lambda_{ex} = 340$ | 4 | Environmental | 20 nM | — | Copper ion | 259 |
| | Commercial carboxylated graphene quantum dot[a] | 353 | ~457–470 | $\lambda_{em,max} = 457$ @ $\lambda_{ex} = 53$ | 4.2 ± 0.8 | Medical | 450 pM | 3–54 nM | Epithelial cell adhesion molecule/EpCAM | 275 |
| Hydrothermal | Hydrosoluble chitosan | 260–450 | ~380–510 | $\lambda_{em,max} = 450$ @ $\lambda_{ex} = 360$ | 3.8 | Environmental | 80 nM | 0–250 µM | Mercury ion | 282 |
| Hydrothermal | Citric acid and tris[b] | 390–440 | ~510 | $\lambda_{em,max} = 510$ @ $\lambda_{ex} = 390$ | 1.5–5 | Medical | 8 nM | 10–70 µM | Hydrogen peroxide | 283 |
| Hydrothermal | Oleic acid and 1-octadecene[c] | 980 | — | — | 27 ± 2 | Medical | 0.5 pM | — | PCA3/mRNA | 276 |
| Modified Hummers method[i] | Graphite powder[d] | 494 | 520 | $\lambda_{em,max} = 520$ @ $\lambda_{ex} = 494$ | 0.8 (thick) | Medical | 3.0 fM | 0.02–100 pM | miRNA-126 | 277 |
| | Commercial carboxyl graphene water dispersion[e] | (1) 485 (2) 634 | (1) 551–620 (2) 660–700 | $\lambda_{em,max} = 520$ @ $\lambda_{ex} = 485$ ; $\lambda_{em,max} = 660$ @ $\lambda_{ex} = 634$ | — | Medical | 2.0 nM, 1.2 nM | — | miRNA-21 miRNA-141 | 278 |
| Commercial graphene oxide[f] | | 460 | ~602 | $\lambda_{em,max} = 602$ @ $\lambda_{ex} = 460$ | — | Medical | 0.76 nM | 3.7–613 nM | Thrombin | 279 |
| Modified Hummer's method[g] | Graphite powder[g] | 495 | ~520 | $\lambda_{em,max} = 520$ @ $\lambda_{ex} = 495$ | 2D flakes µm range[h] | Medical | 0.5 nM | — | Cyclin A$_2$ | 280 |
| Hummer's method | Graphite powder | 480 | ~521 | $\lambda_{em,max} = 521$ @ $\lambda_{ex} = 480$ | — | Medical | 2.5 ng mL$^{-1}$ | 10–150 ng mL$^{-1}$ | MMP-2 | 284 |
| Modified Hummers method | Graphite powder | 240 | ~309 | $\lambda_{em,max} = 309$ @ $\lambda_{ex} = 240$ | — | Medical | 1.3 nM | 1.3–10 nM | Estriol | 281 |
| Modified Hummers method | Graphite powder | 300–500 | 455–495 | $\lambda_{em,max} = 460$ @ $\lambda_{ex} = 360$ | ~2D (H: 2 nm, L < 50) | Medical | 0.6 10 ng mL$^{-1}$ | — | IgG | 285 |

[a] GQD-PEG-aptamer/MoS$_2$ nanocomplex platform. [b] Co-Doped multifunctional carbon dots (N, Zn-CDs) platform. [c] NaYF4:Yb,Er upconversion NPs (UCNPs) as emitters and GO as the fluorescence quencher, GO/UCNP/ssDNA sensing platform. [d] GO/FAM-ssDNA platform as fluorescence sensor based on GO and site-specific DNA cleavage of RsaI endonuclease. [e] Go-Based fluorescence immunosensor including GO/FAM-anti-miR-21/Cy5-anti-miR-141 ssDNA. [f] Hybrid GO-OMO sensing platform, GO-RuQMO-aptamers. [g] Hybrid GO-SWNTs sensing platform, GO/FITC-HAKRRLIF. [h] The SWNTs was 1D nanomaterial, $\phi = 1.1$ nm, length = 50–300 nm. [i] Hummer's method can be similar to chemical ablation regarding synthesis, regarding using the harsh acidic environment (cutting/oxidation).

in PTT investigation. Furthermore, despite other nano-materials, their manufactured CD has acceptable potency in biodistribution, and accumulation exerted from renal filtration in order for clearance from the body of the mouse model. Therefore, their developed CDs are suitable for transfer to clinical biomedical practice.[270] In another study, a novel NIR-II-emitting CD with the quality of triggering by 808 nm laser was manufactured. The synthesised CDs exhibited great properties, such as high luminescence in the 900–1200 nm range, quantum yield (QY of 0.4%) and nontoxicity, which have been suggested to be an effectual agent for NIR-II bioimaging *in vivo* experiments. Their multifunctional probe also showed a great result in photothermal therapy in the tumour animal model with an efficacy of 30.6%, so it can be concluded that the CD-based theragnostic platform has dual functionality in advanced NIR-II bioimaging photothermal therapy of cancer.[271]

PA imaging, which possesses the merits of ultrasound and optical imaging, is a novel promising bioimaging approach with distinctive qualities, including high contrast, superb resolution, and deep-tissue diffusion.[272] Wu *et al.* decorated the surface of porphyrin-implanted CDs with cetuximab, which can distinguish and target cancerous cells with high epidermal growth factor receptor expression so that their nanoparticle can potentially target tumours. The as-synthesised CDs can increase PA amplitude signals and 12 h of signal preservation in the mouse model. So, these CDs can facilitate the prolonged and precise photodynamic therapy of breast cancer tissue.[273]

Parvin and his team synthesised fabricated dual C,N-doped CDs by utilizing ethylene diamine, phosphoric acid and citric acid for carbon and nitrogen. They manufactured a robust strategy to manufacture green and red dual emission P and N co-doped carbon dots (PN-CDs) as PA and fluorescence imaging agents for cancer bioimaging.[274]

### 5.3. Biosensing and chemosensing

In addition to biomedicine and bioimaging, the PL properties of CDs can be used in sensing applications. Since CDs are more biocompatible and less toxic than inorganic quantum dots, they can act as unique optical elements for biosensors and environmentally friendly chemosensors. The main mechanism of sensing in sensors based on CDs originates from the change that is caused at the surface of the CDs in response to the stimulation. The stimulation alters the surface energy states of the CDs. Hence, it affects the fluorescence properties of CDs, such as fluorescence quenching and energy transfer. The fluorescence response of CDs can be either a change in emission intensity and/or an emission shift.

Sidhu *et al.* proposed a complex system comprising CDs and the $Cu^{2+}$ metal cation as a 'turn on' fluorescence sensor for thioredoxin reductase (TrxR) detection in live cell imaging.[259] Inspired by the conjugation affinity of 3-mercaptopropionic acid with $Cu^{2+}$ and the anticancer activity of $Cu^{2+}$, CDs were covalently bound with dithiodipropionic anhydride and the metal cation. Timewise, the sensor responded after 100 min of incubation when a plateau was reached. Shi *et al.* developed a fluorescence resonance energy transfer (FRET) based

biosensor by fabricating a GQD-PEG-aptamer and $MoS_2$ nano-sheet pair to detect the EpCAM protein.[275] The response time of this system for the detection of the EpCAM protein was around 1 h to quantify the fluorescence recovery signals.

In another example, an optical biosensor was created by Vilela *et al.*[276] to detect messenger RNA biomarker PCA3 that is an indicator of prostate cancer. They used upconversion nano-particles (UCNPs) as emitters linked to 25-mer ssDNA as capture probes and graphene oxide (GO) as the fluorescence quencher. Their sensor was tested in different biological media (cell lysis and blood plasma), and the total duration of the test was 1 hour, two times the 30 min incubation of the target analyte and GO. Because of the target-capture DNA hybridization, the UCNPs did not contact GO in the presence of the target PCA3, preserving their fluorescence signal. In another study, a miRNA-126 fluorescence sensor was reported by Tu *et al.*, employing the fluorescence quenching of GO and site-specific cleavage of RsaI endonuclease DNA.[277] The sensing mechanism was based on the fluorescence improvement of the 66-base FAM-labelled ssDNA assembled on GO. This improvement occurred after hybridization of ssDNA with miRNA-126 and cleavage of the dsDNA by RsaI. The average time required for the sensing process (saturated cleavage of dsDNA) was about 2 h.

Several other studies have used low dimensional carbon material as the basis for fluorescent sensors to detect chemical and biological target analytes. These studies are summarized in Table 4. For example, for the diagnosis of prostate cancer, two-colour fluorescence sensors were built by Hizir *et al.* to detect miRNA-21 and miRNA-141 biomarkers in body liquids.[278] Li *et al.*[279] constructed a label-free optical sensing platform for thrombin detection by measuring fluorescence restoration of RuOMO $[Ru(bpy)_2(o\text{-}mopip)]^{2+}$ (bpy = 2,2-bipyridine; *o*-mopip = 2-(2-methoxylphenyl)imidazo[4,5-*f*][1,10]phenanthroline), which was pre-quenched by GO. A cyclin A2 protein, a prognostic indicator for early-stage cancers, was detected using a fluorescence sensor established and developed by Wang *et al.*[280] Kushwaha *et al.*[281] also constructed a fluorescent estriol sensor based on GO's fluorescence enhancement upon bonding to estriol.

## 6. Summary

Nanoparticles, including carbon dots, have already demonstrated enormous potential applications in the area of biomedical and biochemistry. Due to quantum confinement and surface effects, CDs exhibit unique optical properties. In addition, their excellent water solubility, chemical stability, low toxicity, excellent biocompatibility, low cost, and environmental friendliness make them a promising candidate for several applications, such as optical sensing (chemo-/bio-sensing), bioimaging, drug delivery, gene delivery, and theranostics. Despite the increasing interest in the use of CDs since their discovery in 2004,[11,77] their optical properties are not yet fully understood. For instance, the emission in CDs shows a strong dependency on the excitation wavelength. Although this dependency gives flexibility to choose the excitation wavelengths in fluorescence microscopy application, reducing the emission linewidth has been a challenging issue to address. The

control of their emission colour, colour intensity, enhancement of the surface passivation and stabilization of the optical properties are other areas that need to be addressed.

Several routes have been used to synthesise CDs in the forms of CNDs, GQDs, and PDs. A number of these syntheses, including the hydrothermal/solvothermal approach, can be considered an ultimate green chemistry approach toward nontoxic and biocompatible CDs. Despite many efforts undertaken for improving the understanding of CDs from different aspects correlating the synthetic conditions and precursor molecular weight with the reaction outcome, the surface chemistry, morphology, and optical properties (PL) of CDs have not been thoroughly investigated and optimized.

Application-wise, biosensors based on low dimensional carbon materials, including graphene sheets (2D), carbon nanotubes (1D) and CDs (0D), can enhance the current analytical techniques used in research and clinical practice. The various building blocks and many synthetic pathways can make CDs a low-cost chemo-/bio-sensing platform. Additionally, due to the abundant and diverse surface chemistry, the scaffoldings feature in CDs provide easy functionalization routes for many recognition elements for biological sensing. Developing efficient and reliable nanobiosensors (highly sensitive, rapid and target specific), it is vital to improving both recognition and transduction processes by improving the existing materials and techniques. Using CDs, hybrid nanobiosensors can introduce platforms with enhanced signal-to-noise (S/N) ratios by miniaturising the sensor elements.

## Abbreviation

| SQDs | semiconductor quantum dots |
| CNDs | carbon nanodots |
| GQDs | graphene quantum dots |
| PCDs | polymer carbon dots |
| PVA | polyvinyl alcohol |
| DEG | diethylene glycol |
| QY | quantum yield |
| HTC | hydrothermal carbonization |
| PA | photoacoustic therapy |
| PPT | photothermal therapy |

## Author contributions

Mohammadreza Behi conducted the experiments and wrote the paper. Leila Gholami, Sina Naficy finished parts of writing of the paper. Stefano Palomba revised the paper and provided consulting. Fariba Dehghani revised the final version of the paper. All authors have given approval to the final version of the manuscript.

## Conflicts of interest

The authors declare that there is no conflict of interest.

# Acknowledgements

# References

1 C. Ding, A. Zhu and Y. Tian, *Acc. Chem. Res.*, 2014, **47**, 20–30.
2 H. Zhu, H. Zhang and Y. Xia, *Anal. Chem.*, 2018, **90**, 3942–3949.
3 P. Kalisman, Y. Nakibli and L. Amirav, *Nano Lett.*, 2016, **16**, 1776–1781.
4 Z. Cheng, Q. Li, Z. Li, Q. Zhou and Y. Fang, *Nano Lett.*, 2010, **10**, 1864–1868.
5 P. A. Julien, C. Mottillo and T. Friščić, *Green Chem.*, 2017, **19**, 2729–2747.
6 M. L. Liu, B. B. Chen, C. M. Li and C. Z. Huang, *Green Chem.*, 2019, **21**, 449–471.
7 X. Xu, R. Ray, Y. Gu, H. J. Ploehn, L. Gearheart, K. Raker and W. A. Scrivens, *J. Am. Chem. Soc.*, 2004, **126**, 12736–12737.
8 Y. Dong, J. Shao, C. Chen, H. Li, R. Wang, Y. Chi, X. Lin and G. Chen, *Carbon*, 2012, **50**, 4738–4743.
9 P. Luo, Z. Ji, C. Li and G. Shi, *Nanoscale*, 2013, **5**, 7361–7367.
10 H. Li, Z. Kang, Y. Liu and S.-T. Lee, *J. Mater. Chem.*, 2012, **22**, 24230–24253.
11 L. Cao, M. J. Meziani, S. Sahu and Y.-P. Sun, *Acc. Chem. Res.*, 2013, **46**, 171–180.
12 M. Bacon, S. J. Bradley and T. Nann, *Part. Part. Syst. Charact.*, 2014, **31**, 415–428.
13 H. Sun, L. Wu, W. Wei and X. Qu, *Mater. Today*, 2013, **16**, 433–442.
14 X. Yan, B. Li and L.-s. Li, *Acc. Chem. Res.*, 2013, **46**, 2254–2262.
15 Y. Xu, J. Liu, C. Gao and E. Wang, *Electrochem. Commun.*, 2014, **48**, 151–154.
16 S. N. Baker and G. A. Baker, *Angew. Chem., Int. Ed.*, 2010, **49**, 6726–6744.
17 R. Wang, K.-Q. Lu, Z.-R. Tang and Y.-J. Xu, *J. Mater. Chem. A*, 2017, **5**, 3717–3734.
18 H. A. Nguyen, I. Srivastava, D. Pan and M. Gruebele, *ACS Nano*, 2020, **14**, 6127–6137.
19 M. K. Barman and A. Patra, *J. Photochem. Photobiol., C*, 2018, **37**, 1–22.
20 X. Miao, D. Qu, D. Yang, B. Nie, Y. Zhao, H. Fan and Z. Sun, *Adv. Mater.*, 2018, **30**, 1704740.
21 D. Qu, D. Yang, Y. Sun, X. Wang and Z. Sun, *J. Phys. Chem. Lett.*, 2019, **10**, 3849–3857.
22 Y. Su, Y. He, H. Lu, L. Sai, Q. Li, W. Li, L. Wang, P. Shen, Q. Huang and C. Fan, *Biomaterials*, 2009, **30**, 19–25.
23 Y. Su, M. Hu, C. Fan, Y. He, Q. Li, W. Li, L.-h. Wang, P. Shen and Q. Huang, *Biomaterials*, 2010, **31**, 4829–4834.
24 S. Zhu, Q. Meng, L. Wang, J. Zhang, Y. Song, H. Jin, K. Zhang, H. Sun, H. Wang and B. Yang, *Angew. Chem., Int. Ed.*, 2013, **52**, 3953–3957.
25 C. Wang, D. Sun, K. Zhuo, H. Zhang and J. Wang, *RSC Adv.*, 2014, **4**, 54060–54065.

26 Y. Liu, Y. Zhao and Y. Zhang, *Sens. Actuators, B*, 2014, **196**, 647–652.

27 Y.-P. Sun, P. Wang, Z. Lu, F. Yang, M. J. Meziani, G. E. LeCroy, Y. Liu and H. Qian, *Sci. Rep.*, 2015, **5**, 12354.

28 T. Jamieson, R. Bakhshi, D. Petrova, R. Pocock, M. Imani and A. M. Seifalian, *Biomaterials*, 2007, **28**, 4717–4732.

29 S. Y. Lim, W. Shen and Z. Gao, *Chem. Soc. Rev.*, 2015, **44**, 362–381.

30 L. Ai, Y. Yang, B. Wang, J. Chang, Z. Tang, B. Yang and S. Lu, *Sci. Bull.*, 2021, **66**, 839–856.

31 L.-L. Li, J. Ji, R. Fei, C.-Z. Wang, Q. Lu, J.-R. Zhang, L.-P. Jiang and J.-J. Zhu, *Adv. Funct. Mater.*, 2012, **22**, 2971–2979.

32 Y. Dong, H. Pang, H. B. Yang, C. Guo, J. Shao, Y. Chi, C. M. Li and T. Yu, *Angew. Chem., Int. Ed.*, 2013, **52**, 7800–7804.

33 J. Zhang, Y. Yuan, G. Liang and S.-H. Yu, *Adv. Sci.*, 2015, **2**, 1500002.

34 S. Barua, P. K. Raul, R. Gopalakrishnan, B. Das, V. Hmuaka and V. Veer, *ACS Sustainable Chem. Eng.*, 2016, **4**, 2345–2350.

35 C. J. Jeong, A. K. Roy, S. H. Kim, J.-E. Lee, J. H. Jeong, I. In and S. Y. Park, *Nanoscale*, 2014, **6**, 15196–15202.

36 D. Fengyi, Z. Miaomiao, L. Xiaofeng, L. Jianan, J. Xinyi, L. Zhang, H. Ye, S. Genbao, J. Jie, S. Qixiang, Z. Ming and G. Aihua, *Nanotechnology*, 2014, **25**, 315702.

37 S. Sahu, B. Behera, T. K. Maiti and S. Mohapatra, *Chem. Commun.*, 2012, **48**, 8835–8837.

38 L. Wang, B. Li, F. Xu, X. Shi, D. Feng, D. Wei, Y. Li, Y. Feng, Y. Wang, D. Jia and Y. Zhou, *Biosens. Bioelectron.*, 2016, **79**, 1–8.

39 X. Liu, J. Pang, F. Xu and X. Zhang, *Sci. Rep.*, 2016, **6**, 31100.

40 S. Y. Park, H. U. Lee, E. S. Park, S. C. Lee, J.-W. Lee, S. W. Jeong, C. H. Kim, Y.-C. Lee, Y. S. Huh and J. Lee, *ACS Appl. Mater. Interfaces*, 2014, **6**, 3365–3370.

41 Y. Song, S. Zhu and B. Yang, *RSC Adv.*, 2014, **4**, 27184–27200.

42 Z. Yang, Z. Li, M. Xu, Y. Ma, J. Zhang, Y. Su, F. Gao, H. Wei and L. Zhang, *Nano-Micro Lett.*, 2013, **5**, 247–259.

43 Y. Wang and A. Hu, *J. Mater. Chem. C*, 2014, **2**, 6921–6939.

44 X. T. Zheng, A. Ananthanarayanan, K. Q. Luo and P. Chen, *Small*, 2015, **11**, 1620–1636.

45 S. Zhu, Y. Song, X. Zhao, J. Shao, J. Zhang and B. Yang, *Nano Res.*, 2015, **8**, 355–381.

46 R. Das, R. Bandyopadhyay and P. Pramanik, *Mater. Today Chem.*, 2018, **8**, 96–109.

47 X. Zhang, M. Jiang, N. Niu, Z. Chen, S. Li, S. Liu and J. Li, *ChemSusChem*, 2018, **11**, 11–24.

48 G. Hong, S. Diao, A. L. Antaris and H. Dai, *Chem. Rev.*, 2015, **115**, 10816–10906.

49 A. Cayuela, M. L. Soriano, C. Carrillo-Carrion and M. Valcarcel, *Chem. Commun.*, 2016, **52**, 1311–1326.

50 A. Cayuela, M. Soriano, C. Carrillo-Carrión and M. Valcarcel, *Chem. Commun.*, 2016, **52**, 1311–1326.

51 P. Reiss, M. Carrière, C. Lincheneau, L. Vaure and S. Tamang, *Chem. Rev.*, 2016, **116**, 10731–10819.

52 J. Zhou, H. Zhou, J. Tang, S. Deng, F. Yan, W. Li and M. Qu, *Microchim. Acta*, 2017, **184**, 343–368.

53 P. Namdari, B. Negahdari and A. Eatemadi, *Biomed. Pharmacother.*, 2017, **87**, 209–222.

54 M. Tuerhong, X. Yang and Y. Xue-Bo, *Chin. J. Anal. Chem.*, 2017, **45**, 139–150.

55 S. Tao, S. Zhu, T. Feng, C. Xia, Y. Song and B. Yang, *Mater. Today Chem.*, 2017, **6**, 13–25.

56 F. Chen, W. Gao, X. Qiu, H. Zhang, L. Liu, P. Liao, W. Fu and Y. Luo, *Frontiers in Laboratory Medicine*, 2017, **1**, 192–199.

57 K. K. Chan, S. H. K. Yap and K.-T. Yong, *Nano-Micro Lett.*, 2018, **10**, 72.

58 K. Ghosal and A. Ghosh, *Mater. Sci. Eng., C*, 2019, **96**, 887–903.

59 A. M. Wagner, J. M. Knipe, G. Orive and N. A. Peppas, *Acta Biomater.*, 2019, **94**, 44–63.

60 T. Yuan, T. Meng, P. He, Y. Shi, Y. Li, X. Li, L. Fan and S. Yang, *J. Mater. Chem. C*, 2019, **7**, 6820–6835.

61 W. Su, H. Wu, H. Xu, Y. Zhang, Y. Li, X. Li and L. Fan, *Mater. Chem. Front.*, 2020, **4**, 821–836.

62 P. Koutsogiannis, E. Thomou, H. Stamatis, D. Gournis and P. Rudolf, *Adv. Phys.: X*, 2020, **5**, 1758592.

63 R. V. Goreham, Z. Ayed, Z. M. Amin and G. Dobhal, *Nano Futures*, 2020, **4**, 022001.

64 R. Wang, Y. Huang, Y. Chen and Y. Chi, *ACS Appl. Bio Mater.*, 2020, **3**, 6358–6367.

65 Y. Liu, H. Huang, W. Cao, B. Mao, Y. Liu and Z. Kang, *Mater. Chem. Front.*, 2020, **4**, 1586–1613.

66 H. Nie, M. Li, Q. Li, S. Liang, Y. Tan, L. Sheng, W. Shi and S. X.-A. Zhang, *Chem. Mater.*, 2014, **26**, 3104–3112.

67 P. Anilkumar, X. Wang, L. Cao, S. Sahu, J.-H. Liu, P. Wang, K. Korch, K. N. Tackett Ii, A. Parenzan and Y.-P. Sun, *Nanoscale*, 2011, **3**, 2023–2027.

68 L. Cao, X. Wang, M. J. Meziani, F. Lu, H. Wang, P. G. Luo, Y. Lin, B. A. Harruff, L. M. Veca, D. Murray, S.-Y. Xie and Y.-P. Sun, *J. Am. Chem. Soc.*, 2007, **129**, 11318–11319.

69 M. Egorova, A. Tomskaya, K. An and S. Sa, *J. Mater. Sci. Eng.*, 2017, **06**, 5.

70 S. Dolai, S. K. Bhunia, S. Rajendran, V. UshaVipinachandran, S. C. Ray and P. Kluson, *Crit. Rev. Solid State Mater. Sci.*, 2020, 1–22, DOI: 10.1080/10408436.2020.1830750.

71 M. Z. Hu and T. Zhu, *Nanoscale Res. Lett.*, 2015, **10**, 469.

72 X. Ma, S. Li, V. Hessel, L. Lin, S. Meskers and F. Gallucci, *Chem. Eng. Process.*, 2019, **140**, 29–35.

73 W. Liu, R. Liang and Y. Lin, *Nanoscale*, 2020, **12**, 7888–7894.

74 X. Wang, L. Cao, S. T. Yang, F. Lu, M. J. Meziani, L. Tian, K. W. Sun, M. A. Bloodgood and Y. P. Sun, *Angew. Chem.*, 2010, **122**, 5438–5442.

75 W. Kwon, G. Lee, S. Do, T. Joo and S. W. Rhee, *Small*, 2014, **10**, 506–513.

76 C. Liu, P. Zhang, X. Zhai, F. Tian, W. Li, J. Yang, Y. Liu, H. Wang, W. Wang and W. Liu, *Biomaterials*, 2012, **33**, 3604–3613.

77 J. Wang, S. Su, J. Wei, R. Bahgi, L. Hope-Weeks, J. Qiu and S. Wang, *Phys. E*, 2015, **72**, 17.

78 Z. A. Qiao, Q. Huo, M. Chi, G. M. Veith, A. J. Binder and S. Dai, *Adv. Mater.*, 2012, **24**, 6017–6021.

79 S. Zhu, J. Zhang, L. Wang, Y. Song, G. Zhang, H. Wang and B. Yang, *Chem. Commun.*, 2012, **48**, 10889–10891.

80 X. Li, H. Wang, Y. Shimizu, A. Pyatenko, K. Kawaguchi and N. Koshizaki, *Chem. Commun.*, 2011, **47**, 932–934.

81 X. Zhou, Y. Zhang, C. Wang, X. Wu, Y. Yang, B. Zheng, H. Wu, S. Guo and J. Zhang, *ACS Nano*, 2012, **6**, 6592–6599.

82 Y.-F. Mu, W. Zhang, G.-X. Dong, K. Su, M. Zhang and T.-B. Lu, *Small*, 2020, **16**, 2002140.

83 Y. Shin, J. Park, D. Hyun, J. Yang, J.-H. Lee, J.-H. Kim and H. Lee, *Nanoscale*, 2015, **7**, 5633–5637.

84 M. A. Sk, A. Ananthanarayanan, L. Huang, K. H. Lim and P. Chen, *J. Mater. Chem. C*, 2014, **2**, 6954–6960.

85 X. Feng, Z. Li, X. Li and Y. Liu, *Sci. Rep.*, 2016, **6**(1), 33260.

86 D. Li, W. Zhang, X. Yu, Z. Wang, Z. Su and G. Wei, *Nanoscale*, 2016, **8**, 19491–19509.

87 V. Georgakilas, M. Otyepka, A. B. Bourlinos, V. Chandra, N. Kim, K. C. Kemp, P. Hobza, R. Zboril and K. S. Kim, *Chem. Rev.*, 2012, **112**, 6156–6214.

88 R. K. Singh Raman and A. Tiwari, *JOM*, 2014, **66**, 637–642.

89 E. Stolyarova, D. Stolyarov, K. Bolotin, S. Ryu, L. Liu, K. T. Rim, M. Klima, M. Hybertsen, I. Pogorelsky, I. Pavlishin, K. Kusche, J. Hone, P. Kim, H. L. Stormer, V. Yakimenko and G. Flynn, *Nano Lett.*, 2009, **9**, 332–337.

90 X. Feng, Z. Li, X. Li and Y. Liu, *Sci. Rep.*, 2016, **6**, 33260.

91 Z. Zhang, J. Zhang, N. Chen and L. Qu, *Energy Environ. Sci.*, 2012, **5**, 8869–8890.

92 X. T. Zheng, A. Ananthanarayanan, K. Q. Luo and P. Chen, *Small*, 2015, **11**, 1620–1636.

93 L. Tang, R. Ji, X. Cao, J. Lin, H. Jiang, X. Li, K. S. Teng, C. M. Luk, S. Zeng and J. Hao, *ACS Nano*, 2012, **6**, 5102–5110.

94 M. Anju and N. K. Renuka, *Nano-Struct. Nano-Objects*, 2019, **17**, 194–217.

95 Z. Cao, B. Yao, C. Qin, R. Yang, Y. Guo, Y. Zhang, Y. Wu, L. Bi, Y. Chen, Z. Xie, G. Peng, S.-W. Huang, C. W. Wong and Y. Rao, *Light: Sci. Appl.*, 2019, **8**, 107.

96 T. K. Henna and K. Pramod, *Mater. Sci. Eng., C*, 2020, **110**, 110651.

97 M.-L. Chen, Y.-J. He, X.-W. Chen and J.-H. Wang, *Bioconjugate Chem.*, 2013, **24**, 387–397.

98 S. Liu, J. Tian, L. Wang, Y. Zhang, X. Qin, Y. Luo, A. M. Asiri, A. O. Al-Youbi and X. Sun, *Adv. Mater.*, 2012, **24**, 2037–2041.

99 D. Ding, C. C. Goh, G. Feng, Z. Zhao, J. Liu, R. Liu, N. Tomczak, J. Geng, B. Z. Tang and L. G. Ng, *Adv. Mater.*, 2013, **25**, 6083–6088.

100 T. Lai, E. Zheng, L. Chen, X. Wang, L. Kong, C. You, Y. Ruan and X. Weng, *Nanoscale*, 2013, **5**, 8015–8021.

101 Y. Sun, W. Cao, S. Li, S. Jin, K. Hu, L. Hu, Y. Huang, X. Gao, Y. Wu and X.-J. Liang, *Sci. Rep.*, 2013, **3**, 3036.

102 S. Zhu, L. Wang, B. Li, Y. Song, X. Zhao, G. Zhang, S. Zhang, S. Lu, J. Zhang and H. Wang, *Carbon*, 2014, **77**, 462–472.

103 Y. Song, S. Zhu, J. Shao and B. Yang, *J. Polym. Sci., Part A: Polym. Chem.*, 2017, **55**, 610–615.

104 C. Xia, S. Zhu, T. Feng, M. Yang and B. Yang, *Adv. Sci.*, 2019, **6**, 1901316.

105 S. Lu, R. Cong, S. Zhu, X. Zhao, J. Liu, J. S. Tse, S. Meng and B. Yang, *ACS Appl. Mater. Interfaces*, 2016, **8**, 4062–4068.

106 A. Sachdev, I. Matai and P. Gopinath, *Colloids Surf., B*, 2016, **141**, 242–252.

107 Y. Li, Y. Hu, Y. Zhao, G. Shi, L. Deng, Y. Hou and L. Qu, *Adv. Mater.*, 2011, **23**, 776–780.

108 R. Liu, D. Wu, X. Feng and K. Müllen, *J. Am. Chem. Soc.*, 2011, **133**, 15221–15223.

109 M. Pan, X. Xie, K. Liu, J. Yang, L. Hong and S. Wang, *Nanomaterials*, 2020, **10**, 930.

110 K. J. Mintz, Y. Zhou and R. M. Leblanc, *Nanoscale*, 2019, **11**, 4634–4652.

111 J. Kong, N. R. Franklin, C. Zhou, M. G. Chapline, S. Peng, K. Cho and H. Dai, *Science*, 2000, **287**, 622–625.

112 J. Kim and J. S. Suh, *ACS Nano*, 2014, **8**, 4190–4196.

113 Y. Liu, N. Xiao, N. Gong, H. Wang, X. Shi, W. Gu and L. Ye, *Carbon*, 2014, **68**, 258–264.

114 X. Zhai, P. Zhang, C. Liu, T. Bai, W. Li, L. Dai and W. Liu, *Chem. Commun.*, 2012, **48**, 7955–7957.

115 A. B. Bourlinos, A. Stassinopoulos, D. Anglos, R. Zboril, M. Karakassides and E. P. Giannelis, *Small*, 2008, **4**, 455–458.

116 C.-W. Lai, Y.-H. Hsiao, Y.-K. Peng and P.-T. Chou, *J. Mater. Chem.*, 2012, **22**, 14403–14409.

117 X. Wu, F. Tian, W. Wang, J. Chen, M. Wu and J. X. Zhao, *J. Mater. Chem. C*, 2013, **1**, 4676–4684.

118 X. Jia, J. Li and E. Wang, *Nanoscale*, 2012, **4**, 5572–5575.

119 J. Ju and W. Chen, *Biosens. Bioelectron.*, 2014, **58**, 219–225.

120 Y. Deng, D. Zhao, X. Chen, F. Wang, H. Song and D. Shen, *Chem. Commun.*, 2013, **49**, 5751–5753.

121 L. Li, B. Yu and T. You, *Biosens. Bioelectron.*, 2015, **74**, 263–269.

122 H. Huang, Y. Weng, L. Zheng, B. Yao, W. Weng and X. Lin, *J. Colloid Interface Sci.*, 2017, **506**, 373–378.

123 H. Wu, J. Jiang, X. Gu and C. Tong, *Microchim. Acta*, 2017, **184**, 2291–2298.

124 M. K. Kumawat, M. Thakur, R. B. Gurung and R. Srivastava, *ACS Sustainable Chem. Eng.*, 2017, **5**, 1382–1391.

125 D. Crista, J. C. Esteves da Silva and L. Pinto da Silva, *Nanomaterials*, 2020, **10**, 1316.

126 N. Gong, H. Wang, S. Li, Y. Deng, X. a. Chen, L. Ye and W. Gu, *Langmuir*, 2014, **30**, 10933–10939.

127 H. Zhu, X. Wang, Y. Li, Z. Wang, F. Yang and X. Yang, *Chem. Commun.*, 2009, 5118–5120.

128 K.-W. Chu, S. L. Lee, C.-J. Chang and L. Liu, *Polymers*, 2019, **11**, 689.

129 M.-M. Titirici and M. Antonietti, *Chem. Soc. Rev.*, 2010, **39**, 103–116.

130 M. Zhang, L. Hu, H. Wang, Y. Song, Y. Liu, H. Li, M. Shao, H. Huang and Z. Kang, *Nanoscale*, 2018, **10**, 12734–12742.

131 M. N. Egorova, A. E. Tomskaya, A. N. Kapitonov, A. A. Alekseev and S. A. Smagulova, *J. Struct. Chem.*, 2018, **59**, 780–785.

132 J. Song, L. Zhao, Y. Wang, Y. Xue, Y. Deng, X. Zhao and Q. Li, *Nanomaterials*, 2018, **8**, 1043.

133 Y. Yang, J. Cui, M. Zheng, C. Hu, S. Tan, Y. Xiao, Q. Yang and Y. Liu, *Chem. Commun.*, 2012, **48**, 380–382.

134 R. Vikneswaran, R. T subramaniam and R. Yahya, *Mater. Lett.*, 2014, **136**, 179–182.

135 B. De and N. Karak, *RSC Adv.*, 2013, **3**, 8286–8290.

136 L. L. Li, J. Ji, R. Fei, C. Z. Wang, Q. Lu, J. R. Zhang, L. P. Jiang and J. J. Zhu, *Adv. Funct. Mater.*, 2012, **22**, 2971–2979.

137 C. Xia, S. Zhu, T. Feng, M. Yang and B. Yang, *Adv. Sci.*, 2019, **6**, 1901316.

138 S. Tajik, Z. Dourandish, K. Zhang, H. Beitollahi, Q. V. Le, H. W. Jang and M. Shokouhimehr, *RSC Adv.*, 2020, **10**, 15406–15429.

139 A. Sharma and J. Das, *J. Nanobiotechnol.*, 2019, **17**, 92.

140 M. Zheng, S. Ruan, S. Liu, T. Sun, D. Qu, H. Zhao, Z. Xie, H. Gao, X. Jing and Z. Sun, *ACS Nano*, 2015, **9**, 11455–11461.

141 Z.-A. Qiao, Y. Wang, Y. Gao, H. Li, T. Dai, Y. Liu and Q. Huo, *Chem. Commun.*, 2010, **46**, 8812–8814.

142 H. Li, X. He, Z. Kang, H. Huang, Y. Liu, J. Liu, S. Lian, C. H. A. Tsang, X. Yang and S. T. Lee, *Angew. Chem., Int. Ed.*, 2010, **49**, 4430–4434.

143 J. Peng, W. Gao, B. K. Gupta, Z. Liu, R. Romero-Aburto, L. Ge, L. Song, L. B. Alemany, X. Zhan and G. Gao, *Nano Lett.*, 2012, **12**, 844–849.

144 D. B. Shinde and V. K. Pillai, *Chem.–Eur. J.*, 2012, **18**, 12522–12528.

145 Y. Dong, C. Chen, X. Zheng, L. Gao, Z. Cui, H. Yang, C. Guo, Y. Chi and C. M. Li, *J. Mater. Chem.*, 2012, **22**, 8764–8766.

146 Q. Wang, H. Zheng, Y. Long, L. Zhang, M. Gao and W. Bai, *Carbon*, 2011, **49**, 3134–3140.

147 H. Liu, T. Ye and C. Mao, *Angew. Chem., Int. Ed.*, 2007, **46**, 6473–6475.

148 J. Lu, J.-x. Yang, J. Wang, A. Lim, S. Wang and K. P. Loh, *ACS Nano*, 2009, **3**, 2367–2375.

149 L. Zheng, Y. Chi, Y. Dong, J. Lin and B. Wang, *J. Am. Chem. Soc.*, 2009, **131**, 4564–4565.

150 D. Pan, J. Zhang, Z. Li and M. Wu, *Adv. Mater.*, 2010, **22**, 734–738.

151 S. Zhu, J. Zhang, C. Qiao, S. Tang, Y. Li, W. Yuan, B. Li, L. Tian, F. Liu and R. Hu, *Chem. Commun.*, 2011, **47**, 6858–6860.

152 L. Lin and S. Zhang, *Chem. Commun.*, 2012, **48**, 10177–10179.

153 M. Bottini, C. Balasubramanian, M. I. Dawson, A. Bergamaschi, S. Bellucci and T. Mustelin, *J. Phys. Chem. B*, 2006, **110**, 831–836.

154 Y.-P. Sun, B. Zhou, Y. Lin, W. Wang, K. S. Fernando, P. Pathak, M. J. Meziani, B. A. Harruff, X. Wang and H. Wang, *J. Am. Chem. Soc.*, 2006, **128**, 7756–7757.

155 L. Fan, M. Zhu, X. Lee, R. Zhang, K. Wang, J. Wei, M. Zhong, D. Wu and H. Zhu, *Part. Part. Syst. Charact.*, 2013, **30**, 764–769.

156 J. Lee, K. Kim, W. I. Park, B.-H. Kim, J. H. Park, T.-H. Kim, S. Bong, C.-H. Kim, G. Chae and M. Jun, *Nano Lett.*, 2012, **12**, 6078–6083.

157 H. Sun, N. Gao, L. Wu, J. Ren, W. Wei and X. Qu, *Chem.–Eur. J.*, 2013, **19**, 13362–13368.

158 Y. Li, Y. Hu, Y. Zhao, G. Shi, L. Deng, Y. Hou and L. Qu, *Adv. Mater.*, 2011, **23**, 776–780.

159 A. Ananthanarayanan, X. Wang, P. Routh, B. Sana, S. Lim, D. H. Kim, K. H. Lim, J. Li and P. Chen, *Adv. Funct. Mater.*, 2014, **24**, 3021–3026.

160 Q.-L. Zhao, Z.-L. Zhang, B.-H. Huang, J. Peng, M. Zhang and D.-W. Pang, *Chem. Commun.*, 2008, 5116–5118.

161 L. Bao, Z. L. Zhang, Z. Q. Tian, L. Zhang, C. Liu, Y. Lin, B. Qi and D. W. Pang, *Adv. Mater.*, 2011, **23**, 5801–5806.

162 J. Deng, Q. Lu, N. Mi, H. Li, M. Liu, M. Xu, L. Tan, Q. Xie, Y. Zhang and S. Yao, *Chem.–Eur. J.*, 2014, **20**, 4993–4999.

163 P. Yu, S. E. Lowe, G. P. Simon and Y. L. Zhong, *Curr. Opin. Colloid Interface Sci.*, 2015, **20**, 329–338.

164 Z. L. Wu, Z. X. Liu and Y. H. Yuan, *J. Mater. Chem. B*, 2017, **5**, 3794–3809.

165 J. Zuo, T. Jiang, X. Zhao, X. Xiong, S. Xiao and Z. Zhu, *J. Nanomater.*, 2015, **2015**, 787862.

166 Y. Song, K. Qu, C. Zhao, J. Ren and X. Qu, *Adv. Mater.*, 2010, **22**, 2206–2210.

167 J. Liu and Y. Lu, *J. Am. Chem. Soc.*, 2003, **125**, 6642–6643.

168 H. Peng and J. Travas-Sejdic, *Chem. Mater.*, 2009, **21**, 5563–5565.

169 H. Li, X. He, Z. Kang, H. Huang, Y. Liu, J. Liu, S. Lian, C. H. Tsang, X. Yang and S. T. Lee, *Angew. Chem., Int. Ed. Engl.*, 2010, **49**, 4430–4434.

170 J. Zhou, C. Booker, R. Li, X. Zhou, T. K. Sham, X. Sun and Z. Ding, *J. Am. Chem. Soc.*, 2007, **129**, 744–745.

171 D. B. Shinde and V. K. Pillai, *Chemistry*, 2012, **18**, 12522–12528.

172 L. Bao, Z. L. Zhang, Z. Q. Tian, L. Zhang, C. Liu, Y. Lin, B. Qi and D. W. Pang, *Adv. Mater.*, 2011, **23**, 5801–5806.

173 J. Deng, Q. Lu, N. Mi, H. Li, M. Liu, M. Xu, L. Tan, Q. Xie, Y. Zhang and S. Yao, *Chemistry*, 2014, **20**, 4993–4999.

174 C. Dowding, in *Advances in Laser Materials Processing*, ed. J. Lawrence, J. Pou, D. K. Y. Low and E. Toyserkani, Woodhead Publishing, 2010, pp. 575–628, DOI: DOI: 10.1533/9781845699819.7.575.

175 Y. P. Sun, B. Zhou, Y. Lin, W. Wang, K. A. Fernando, P. Pathak, M. J. Meziani, B. A. Harruff, X. Wang, H. Wang, P. G. Luo, H. Yang, M. E. Kose, B. Chen, L. M. Veca and S. Y. Xie, *J. Am. Chem. Soc.*, 2006, **128**, 7756–7757.

176 L. Cao, X. Wang, M. J. Meziani, F. Lu, H. Wang, P. G. Luo, Y. Lin, B. A. Harruff, L. M. Veca, D. Murray, S. Y. Xie and Y. P. Sun, *J. Am. Chem. Soc.*, 2007, **129**, 11318–11319.

177 S.-L. Hu, K.-Y. Niu, J. Sun, J. Yang, N.-Q. Zhao and X.-W. Du, *J. Mater. Chem.*, 2009, **19**, 484–488.

178 F. Du, F. Zeng, Y. Ming and S. Wu, *Microchim. Acta*, 2013, **180**, 453–460.

179 S. C. Ray, A. Saha, N. R. Jana and R. Sarkar, *J. Phys. Chem. C*, 2009, **113**, 18546–18551.

180 X. Sun, Z. Liu, K. Welsher, J. T. Robinson, A. Goodwin, S. Zaric and H. Dai, *Nano Res.*, 2008, **1**, 203–212.

181 L. Tian, D. Ghosh, W. Chen, S. Pradhan, X. Chang and S. Chen, *Chem. Mater.*, 2009, **21**, 2803–2809.

182 L. Shen, L. Zhang, M. Chen, X. Chen and J. Wang, *Carbon*, 2013, **55**, 343–349.

183 Y. Dong, N. Zhou, X. Lin, J. Lin, Y. Chi and G. Chen, *Chem. Mater.*, 2010, **22**, 5895–5899.

184 J. Shen, Y. Zhu, C. Chen, X. Yang and C. Li, *Chem. Commun.*, 2011, **47**, 2580–2582.

185 S. Zhu, Q. Meng, L. Wang, J. Zhang, Y. Song, H. Jin, K. Zhang, H. Sun, H. Wang and B. Yang, *Angew. Chem.*, 2013, **125**, 4045–4049.

186 Z. Zhang, J. Hao, J. Zhang, B. Zhang and J. Tang, *RSC Adv.*, 2012, **2**, 8599–8601.

187 S. K. Bhunia, A. Saha, A. R. Maity, S. C. Ray and N. R. Jana, *Sci. Rep.*, 2013, **3**, 1473.

188 Z.-C. Yang, M. Wang, A. M. Yong, S. Y. Wong, X.-H. Zhang, H. Tan, A. Y. Chang, X. Li and J. Wang, *Chem. Commun.*, 2011, **47**, 11615–11617.

189 H. Liu, Z. Li, Y. Sun, X. Geng, Y. Hu, H. Meng, J. Ge and L. Qu, *Sci. Rep.*, 2018, **8**, 1086.

190 X. Miao, D. Qu, D. Yang, B. Nie, Y. Zhao, H. Fan and Z. Sun, *Adv. Mater.*, 2018, **30**, 1704740.

191 A. M. Senol and E. Bozkurt, *Microchem. J.*, 2020, **159**, 105357.

192 D. K. Dang, C. Sundaram, Y.-L. T. Ngo, J. S. Chung, E. J. Kim and S. H. Hur, *Sens. Actuators, B*, 2018, **255**, 3284–3291.

193 A. Iqbal, K. Iqbal, L. Xu, B. Li, D. Gong, X. Liu, Y. Guo, W. Liu, W. Qin and H. Guo, *Sens. Actuators, B*, 2018, **255**, 1130–1138.

194 A. Iqbal, Y. Tian, X. Wang, D. Gong, Y. Guo, K. Iqbal, Z. Wang, W. Liu and W. Qin, *Sens. Actuators, B*, 2016, **237**, 408–415.

195 I. P.-J. Lai, S. G. Harroun, S.-Y. Chen, B. Unnikrishnan, Y.-J. Li and C.-C. Huang, *Sens. Actuators, B*, 2016, **228**, 465–470.

196 Ł. Janus, J. Radwan-Pragłowska, M. Piątkowski and D. Bogdał, *Materials*, 2020, **13**, 3313.

197 M. Ge, X. Huang, J. Ni, Y. Han, C. Zhang, S. Li, J. Cao, J. Li, Z. Chen and S. Han, *Dyes Pigm.*, 2020, 108953.

198 J.-H. Zhou, J.-P. He, Y.-J. Ji, W.-J. Dang, X.-L. Liu, G.-W. Zhao, C.-X. Zhang, J.-S. Zhao, Q.-B. Fu and H.-P. Hu, *Electrochim. Acta*, 2007, **52**, 4691–4695.

199 Y. Yang, B. Zhao, Y. Gao, H. Liu, Y. Tian, D. Qin, H. Wu, W. Huang and L. Hou, *Nano-Micro Lett.*, 2015, **7**, 325–331.

200 F. Niu, Y. Xu, J. Liu, Z. Song, M. Liu and J. Liu, *Electrochim. Acta*, 2017, **236**, 239–251.

201 X. Liu, J. Pang, F. Xu and X. Zhang, *Sci. Rep.*, 2016, **6**, 31100.

202 S. Ahirwar, S. Mallick and D. Bahadur, *ACS Omega*, 2017, **2**, 8343–8353.

203 X. Wang, K. Qu, B. Xu, J. Ren and X. Qu, *J. Mater. Chem.*, 2011, **21**, 2445–2450.

204 J. Jiang, Y. He, S. Li and H. Cui, *Chem. Commun.*, 2012, **48**, 9634–9636.

205 T. V. de Medeiros, J. Manioudakis, F. Noun, J.-R. Macairan, F. Victoria and R. Naccache, *J. Mater. Chem. C*, 2019, **7**, 7175–7195.

206 K. M. Omer, K. H. Hama Aziz, Y. M. Salih, D. I. Tofiq and A. Q. Hassan, *New J. Chem.*, 2019, **43**, 689–695.

207 A. Başoğlu, Ü. Ocak and A. Gümrükçüoğlu, *J. Fluoresc.*, 2020, **30**, 515–526.

208 T. Yu, H. Wang, C. Guo, Y. Zhai, J. Yang and J. Yuan, *R. Soc. Open Sci.*, 2018, **5**, 180245.

209 Y.-P. Sun, B. Zhou, Y. Lin, W. Wang, K. S. Fernando, P. Pathak, M. J. Meziani, B. A. Harruff, X. Wang and H. Wang, *J. Am. Chem. Soc.*, 2006, **128**, 7756–7757.

210 X. Li, H. Wang, Y. Shimizu, A. Pyatenko, K. Kawaguchi and N. Koshizaki, *Chem. Commun.*, 2010, **47**, 932–934.

211 H. P. S. Castro, V. S. Souza, J. D. Scholten, J. H. Dias, J. A. Fernandes, F. S. Rodembusch, R. dosReis, J. Dupont, S. R. Teixeira and R. R. B. Correia, *Chem.–Eur. J.*, 2016, **22**, 138–143.

212 H. Castro, V. Souza, J. Scholten, J. Dias, J. Alves Fernandes, F. Rodembusch, R. Dos Reis, J. Dupont, S. Teixeira and R. Correia, *Chemistry*, Weinheim an der Bergstrasse, Germany, 2015, vol. 22.

213 C. Doñate-Buendia, R. Torres-Mendieta, A. Pyatenko, E. Falomir, M. Fernández-Alonso and G. Mínguez-Vega, *ACS Omega*, 2018, **3**, 2735–2742.

214 L. Lin, S. A. Starostin, S. Li, S. A. Khan and V. Hessel, *Chem. Eng. Sci.*, 2018, **178**, 157–166.

215 L. Lin and Q. Wang, *Plasma Chem. Plasma Process.*, 2015, **35**, 925–962.

216 X. Ma, S. Li, V. Hessel, L. Lin, S. Meskers and F. Gallucci, *Chem. Eng. Sci.*, 2020, **220**, 115648.

217 C. Chokradjaroen, S. Theeramunkong, H. Yui, N. Saito and R. Rujiravanit, *Carbohydr. Polym.*, 2018, **201**, 20–30.

218 T. Morishita, T. Ueno, G. Panomsuwan, J. Hieda, A. Yoshida, M. A. Bratescu and N. Saito, *Sci. Rep.*, 2016, **6**, 36880.

219 M. O. Dekaliuk, O. Viagin, Y. V. Malyukin and A. P. Demchenko, *Phys. Chem. Chem. Phys.*, 2014, **16**, 16075–16084.

220 M. J. Krysmann, A. Kelarakis, P. Dallas and E. P. Giannelis, *J. Am. Chem. Soc.*, 2011, **134**, 747–750.

221 C. T. Chien, S. S. Li, W. J. Lai, Y. C. Yeh, H. A. Chen, I. Chen, L. C. Chen, K. H. Chen, T. Nemoto and S. Isoda, *Angew. Chem., Int. Ed.*, 2012, **51**, 6662–6666.

222 B. Zhi, X. Yao, Y. Cui, G. Orr and C. L. Haynes, *Nanoscale*, 2019, **11**, 20411–20428.

223 O. Kozák, M. Sudolská, G. Pramanik, P. Cígler, M. Otyepka and R. Zbořil, *Chem. Mater.*, 2016, **28**, 4085–4128.

224 J. Zhu, X. Bai, X. Chen, H. Shao, Y. Zhai, G. Pan, H. Zhang, E. V. Ushakova, Y. Zhang, H. Song and A. L. Rogach, *Adv. Opt. Mater.*, 2019, **7**, 1801599.

225 F. Yuan, T. Yuan, L. Sui, Z. Wang, Z. Xi, Y. Li, X. Li, L. Fan, Z. a. Tan, A. Chen, M. Jin and S. Yang, *Nat. Commun.*, 2018, **9**, 2249.

226 K. Jiang, X. Feng, X. Gao, Y. Wang, C. Cai, Z. Li and H. Lin, *Nanomaterials*, 2019, **9**, 529.

227 S. Hu, A. Trinchi, P. Atkin and I. Cole, *Angew. Chem., Int. Ed. Engl.*, 2015, **54**, 2970–2974.

228 H. Ding, S.-B. Yu, J.-S. Wei and H.-M. Xiong, *ACS Nano*, 2016, **10**, 484–491.

229 Y. Xiong, J. Schneider, E. V. Ushakova and A. L. Rogach, *Nano Today*, 2018, **23**, 124–139.

230 K. Mishra, S. Koley and S. Ghosh, *J. Phys. Chem. Lett.*, 2019, **10**, 335–345.

231 M. Shamsipur, A. Barati, A. A. Taherpour and M. Jamshidi, *J. Phys. Chem. Lett.*, 2018, **9**, 4189–4198.

232 T. Zhang, J. Zhu, Y. Zhai, H. Wang, X. Bai, B. Dong, H. Wang and H. Song, *Nanoscale*, 2017, **9**, 13042–13051.

233 J. B. Essner, J. A. Kist, L. Polo-Parada and G. A. Baker, *Chem. Mater.*, 2018, **30**, 1878–1887.

234 Y. Wang and A. Hu, *J. Mater. Chem. C*, 2014, **2**, 6921–6939.

235 Z. Kang and Y. Liu, in *Carbon Nanoparticles and Nanostructures*, ed. N. Yang, X. Jiang and D.-W. Pang, Springer International Publishing, Cham, 2016, pp. 257-298, DOI: 10.1007/978-3-319-28782-9_8.

236 S. Soley, *Carbon Quantum Dots: Synthesis and Optronics Applications*, 2017.

237 R. Shereema, T. Sruthi, V. S. Kumar, T. Rao and S. S. Shankar, *Biochemistry*, 2015, **54**, 6352–6356.

238 P. Wu, Y. Pan, J. Yan, D. Huang and S. Li, *Molecules*, 2016, **21**, 106.

239 Y. Zhao, Y. Zhang, X. Liu, H. Kong, Y. Wang, G. Qin, P. Cao, X. Song, X. Yan, Q. Wang and H. Qu, *Sci. Rep.*, 2017, **7**, 4452.

240 M. Zhang, Y. Zhao, J. Cheng, X. Liu, Y. Wang, X. Yan, Y. Zhang, F. Lu, Q. Wang and H. Qu, *Artif. Cells, Nanomed., Biotechnol.*, 2018, **46**, 1562–1571.

241 Y. Xu, B. Wang, H. Zhang, X. Qu, M. Zhang, X. An, S. Lu and S. Zhang, *Blood*, 2019, **134**, 941.

242 J. Xia, Y. Kawamura, T. Suehiro, Y. Chen and K. Sato, *Drug Discoveries Ther.*, 2019, **13**, 114–117.

243 J. Chen, Q. Wang, J. Zhou, W. Deng, Q. Yu, X. Cao, J. Wang, F. Shao, Y. Li, P. Ma, M. Spector, J. Yu and X. Xu, *Nanoscale*, 2017, **9**, 10820–10831.

244 M. Zhang, X. Zhao, Z. Fang, Y. Niu, J. Lou, Y. Wu, S. Zou, S. Xia, M. Sun and F. Du, *RSC Adv.*, 2017, **7**, 3369–3375.

245 A. Rezaei and E. Hashemi, *Sci. Rep.*, 2021, **11**, 13790.

246 H. Ding, F. Du, P. Liu, Z. Chen and J. Shen, *ACS Appl. Mater. Interfaces*, 2015, **7**, 6889–6897.

247 B. Wang, S. Wang, Y. Wang, Y. Lv, H. Wu, X. Ma and M. Tan, *Biotechnol. Lett.*, 2016, **38**, 191–201.

248 T. Kong, L. Hao, Y. Wei, X. Cai and B. Zhu, *Cell Proliferation*, 2018, **51**, e12488.

249 M. Zheng, S. Liu, J. Li, D. Qu, H. Zhao, X. Guan, X. Hu, Z. Xie, X. Jing and Z. Sun, *Adv. Mater.*, 2014, **26**, 3554–3560.

250 S. L. D'souza, S. S. Chettiar, J. R. Koduru and S. K. Kailasa, *Optik*, 2018, **158**, 893–900.

251 M. Z. Fahmi, A. Haris, A. J. Permana, D. L. N. Wibowo, B. Purwanto, Y. L. Nikmah and A. Idris, *RSC Adv.*, 2018, **8**, 38376–38383.

252 S. Nandi, R. Malishev, K. P. Kootery, Y. Mirsky, S. Kolusheva and R. Jelinek, *Chem. Commun.*, 2014, **50**, 10299–10302.

253 L. Lu, C. Feng, J. Xu, F. Wang, H. Yu, Z. Xu and W. Zhang, *Biosens. Bioelectron.*, 2017, **92**, 101–108.

254 W.-Q. Li, Z. Wang, S. Hao, L. Sun, M. Nisic, G. Cheng, C. Zhu, Y. Wan, L. Ha and S.-Y. Zheng, *Nanoscale*, 2018, **10**, 3744–3752.

255 R. Jelinek, *Carbon Quantum Dots*, 2017.

256 K. Jiang, S. Sun, L. Zhang, Y. Lu, A. Wu, C. Cai and H. Lin, *Angew. Chem., Int. Ed.*, 2015, **54**, 5360–5363.

257 S. K. Bhunia, S. Nandi, R. Shikler and R. Jelinek, *Nanoscale*, 2016, **8**, 3400–3406.

258 Y. Chen, M. Zheng, Y. Xiao, H. Dong, H. Zhang, J. Zhuang, H. Hu, B. Lei and Y. Liu, *Adv. Mater.*, 2016, **28**, 312–318.

259 J. S. Sidhu, A. Singh, N. Garg, N. Kaur and N. Singh, *Analyst*, 2018, **143**, 1853–1861.

260 B. Murugesan, J. Sonamuthu, N. Pandiyan, B. Pandi, S. Samayanan and S. Mahalingam, *J. Photochem. Photobiol., B*, 2018, **178**, 371–379.

261 Y. Sun, S. Zheng, L. Liu, Y. Kong, A. Zhang, K. Xu and C. Han, *Nanoscale Res. Lett.*, 2020, **15**, 55.

262 U. Sivasankaran, S. Jesny, A. R. Jose and K. Girish Kumar, *Anal. Sci.*, 2017, **33**, 281–285.

263 C. Dias, N. Vasimalai, M. P Sárria, I. Pinheiro, V. Vilas-Boas, J. Peixoto and B. Espiña, *Nanomaterials*, 2019, **9**, 199.

264 Y. Song, X. Yan, Z. Li, L. Qu, C. Zhu, R. Ye, S. Li, D. Du and Y. Lin, *J. Mater. Chem. B*, 2018, **6**, 3181–3187.

265 Y. Liu, K. Ai, J. Liu, M. Deng, Y. He and L. Lu, *Adv. Mater.*, 2013, **25**, 1353–1359.

266 L. V. Wang and S. Hu, *science*, 2012, **335**, 1458–1462.

267 A. M. Smith, M. C. Mancini and S. Nie, *Nat. Nanotechnol.*, 2009, **4**, 710–711.

268 J. An, C. M. Shade, D. A. Chengelis-Czegan, S. Petoud and N. L. Rosi, *J. Am. Chem. Soc.*, 2011, **133**, 1220–1223.

269 Y. Lyu, C. Xie, S. A. Chechetka, E. Miyako and K. Pu, *J. Am. Chem. Soc.*, 2016, **138**, 9049–9052.

270 X. Bao, Y. Yuan, J. Chen, B. Zhang, D. Li, D. Zhou, P. Jing, G. Xu, Y. Wang, K. Holá, D. Shen, C. Wu, L. Song, C. Liu, R. Zbořil and S. Qu, *Light: Sci. Appl.*, 2018, **7**, 91.

271 Y. Li, G. Bai, S. Zeng and J. Hao, *ACS Appl. Mater. Interfaces*, 2019, **11**, 4737–4744.

272 A. Gaiduk, M. Yorulmaz, P. Ruijgrok and M. Orrit, *Science*, 2010, **330**, 353–356.

273 F. Wu, H. Su, Y. Cai, W.-K. Wong, W. Jiang and X. Zhu, *ACS Appl. Bio Mater.*, 2018, **1**, 110–117.

274 N. Parvin and T. K. Mandal, *Microchim. Acta*, 2017, **184**, 1117–1125.

275 J. Shi, J. Lyu, F. Tian and M. Yang, *Biosens. Bioelectron.*, 2017, **93**, 182–188.

276 P. Vilela, A. El-Sagheer, T. M. Millar, T. Brown, O. L. Muskens and A. G. Kanaras, *ACS Sens.*, 2016, **2**, 52–56.

277 Y. Tu, W. Li, P. Wu, H. Zhang and C. Cai, *Anal. Chem.*, 2013, **85**, 2536–2542.

278 M. S. Hizir, M. Balcioglu, M. Rana, N. M. Robertson and M. V. Yigit, *ACS Appl. Mater. Interfaces*, 2014, **6**, 14772–14778.

279 J. Li, X. Hu, S. Shi, Y. Zhang and T. Yao, *J. Mater. Chem. B*, 2016, **4**, 1361–1367.

280 X. Wang, C. Wang, K. Qu, Y. Song, J. Ren, D. Miyoshi, N. Sugimoto and X. Qu, *Adv. Funct. Mater.*, 2010, **20**, 3967–3971.

281 H. Kushwaha, R. Sao and R. Vaish, *J. Appl. Phys.*, 2014, **116**, 034701.

282 L. Wang, B. Li, F. Xu, X. Shi, D. Feng, D. Wei, Y. Li, Y. Feng, Y. Wang and D. Jia, *Biosens. Bioelectron.*, 2016, **79**, 1–8.

283 P. Das, S. Ganguly, M. Bose, S. Mondal, S. Choudhary, S. Gangopadhyay, A. K. Das, S. Banerjee and N. C. Das, *Mater. Sci. Eng., C*, 2018, **88**, 115–129.

284 E. Song, D. Cheng, Y. Song, M. Jiang, J. Yu and Y. Wang, *Biosens. Bioelectron.*, 2013, **47**, 445–450.

285 H. Zhao, Y. Chang, M. Liu, S. Gao, H. Yu and X. Quan, *Chem. Commun.*, 2013, **49**, 234–236.